

Development of Push Control Strategy for Diesel-Electric Powertrains

Johannes Bodin

Master of Science Thesis in Electrical Engineering
Development of Push Control Strategy for Diesel-Electric Powertrains

Johannes Bodin

LiTH-ISY-EX--18/5168--SE

Supervisor: **Viktor Leek**
ISY, Linköping University
Mats Nordlöf
BAE Systems Hägglunds AB, Örnköldsvik

Examiner: **Lars Eriksson**
ISY, Linköping University

*Division of Vehicular Systems
Department of Electrical Engineering
Linköping University
SE-581 83 Linköping, Sweden*

Copyright © 2018 Johannes Bodin

Abstract

In diesel-electric powertrains, the wheels are mechanically decoupled from the internal combustion engine (ICE). The conventional control approach for such a powertrain is to let the driver control the traction motor while the ICE realizes speed control, causing power to be *pulled* through the powertrain. An alternative approach is to *push* power forward by letting the driver control the ICE instead. In this thesis, a conceptual simulation model of a diesel-electric powertrain is compiled and the characteristics of this novel approach investigated. It is concluded that the new approach makes full ICE power utilization possible even with engine performance reductions present, and also that it handles load prioritization in a natural way. However, takeoff from standstill and low-speed driving become difficult due to the effective gear ratio growing towards infinity for decreasing vehicle speed, causing high traction torques at low speed.

Acknowledgments

I would first of all like to thank BAE Systems Hägglunds in Örnsköldsvik for giving me the opportunity to carry out this exciting thesis work in cooperation with you. Special thanks to my supervisor Mats Nordlöf for invaluable support along the way. I am truly grateful for your guidance through the interesting but dense jungle of powertrain control, and for the excellent way of introducing the scary thing called "reality" to my former, rather ideal picture of the world of control.

Thanks also to my examiner Lars Eriksson and my supervisor Viktor Leek at Linköping University for your much appreciated contributions and helpful attitudes.

Additionally, I would like to thank my fellow thesis workers at Hägglunds (Carolin, Simon, Johan, Viktor, Alexander, Erik and Linus) for an enjoyable semester. Who knows, maybe the ideas from our interesting coffee break discussions about AI powered kitchen utils and W26 engines will come handy as inspiration one day?

Finally, I want to send the warmest of thanks to my family and friends for your love and support during the thesis work.

Örnsköldsvik, August 2018
Johannes Bodin

Contents

Notation	xi
1 Introduction	1
1.1 Motivation	1
1.2 Purpose	2
1.3 Problem formulation	2
1.4 Delimitations	2
1.5 Requirements	3
1.6 Outline	3
2 The Diesel-Electric Powertrain	5
2.1 System description	7
2.2 Control	8
2.2.1 ECU	8
2.2.2 GCU & TCU	9
2.2.3 Control limitations due to subsystem boundaries	10
2.3 Communication	10
2.4 Established control strategy (CS1)	10
2.4.1 Torque reduction	10
2.4.2 Pull analogy	11
2.4.3 Maximum power utilization problem	12
2.5 Proposed control strategy (CS2)	13
2.5.1 Push analogy	13
3 Approach	15
3.1 Drive cycles	17
3.1.1 Fictive drive cycle	17
3.1.2 Real drive cycle	18
4 Related Research	19
4.1 Control	19
4.2 Modeling	20

5	Modeling	23
5.1	Internal combustion engine	23
5.1.1	States and control inputs	23
5.1.2	Internal signals and outputs	24
5.1.3	State and control signal normalization	25
5.1.4	Maximum torque limit	25
5.2	ECU	25
5.2.1	Fuel feed-forward	25
5.2.2	Smoke limiter	25
5.2.3	Low idle governor	26
5.2.4	Wastegate control	26
5.3	Genset shaft	27
5.4	Generator, traction motor & inverters	27
5.5	GCU/TCU	27
5.6	DC bus	28
5.7	Drive shaft & vehicle	29
5.7.1	Simplified loss assumption	29
5.7.2	Reflected inertia	29
5.8	Bus communication	29
5.9	Model validation	30
5.9.1	ECU & ICE	30
5.9.2	GCU/TCU	31
5.9.3	Complete powertrain	33
6	Control Strategy Development	35
6.1	Proposed strategy (CS2)	35
6.1.1	Voltage control at standstill	35
6.1.2	Voltage control at no traction demand	35
6.1.3	Power path analysis	36
6.2	Control loop migration to PCM	38
6.2.1	Feasibility	38
6.3	Alternative strategy (CS3)	38
6.3.1	Initial idea	39
6.3.2	Variable effective controller gains	40
6.4	Gear ratio compensated control signal	41
6.4.1	Deceleration from 20 km/h to standstill	41
6.4.2	Full drive cycle	42
6.5	Friction and pump loss compensation	44
6.5.1	Engine braking	44
6.6	Speed reference selection	46
6.6.1	Reference directly from map	46
6.6.2	Limited shaft acceleration torque	48
6.7	Traction power limit with ICE torque reduction	51
6.8	Conditional idle speed setting	54
6.9	Infinite torque gain	56
6.9.1	Takeoff strategy	56

7	Results	59
7.1	Final control strategy	59
7.1.1	Parameters	59
7.2	Simulation results	61
7.2.1	Fictive drive cycle, 100% ICE performance	62
7.2.2	Fictive drive cycle, 70% ICE performance	63
7.2.3	Real drive cycle	64
8	Discussion	65
8.1	Results	65
8.1.1	Jerks during real drive cycle	65
8.1.2	Natural priority handling	66
8.1.3	Uncertain applicability of real drive cycle signals	66
8.2	Modeling	67
8.2.1	Limited model validation	67
8.2.2	Simplified component models	67
8.3	General discussion	68
8.3.1	Speed control dynamics affecting traction	68
8.3.2	Driver interpretation using traction torque	68
8.3.3	CS1 with control loop migration	68
8.3.4	Benefits of energy storage	69
9	Conclusions & Future Work	71
9.1	Conclusions	71
9.2	Future work	72
9.2.1	Speed reference selection algorithm	72
9.2.2	Takeoff strategy	73
9.2.3	Improved model validation	73
9.2.4	Extended fictive drive cycle	73
	Bibliography	75

Notation

ABBREVIATIONS

Abbreviation	Meaning
AUX	Auxiliary
CAN	Controller Area Network
CS{x}	Control Strategy {x}
CU	Control Unit
GCU	Generator Control Unit
GEN	Generator
GENSET	Engine-Generator Set
ECU	Engine Control Unit
EM	Electric Machine
FOC	Field Oriented Control
ICE	Internal Combustion Engine
LIG	Low Idle Governor
MVEM	Mean Value Engine Model
PAR	Parasitic
PCM	Powertrain Control Module
SAE	Society of Automotive Engineers
SHEV	Series Hybrid Electric Vehicle
TCU	Traction Control Unit
TM	Traction Motor

MODEL RELATED NOTATION

Notation	Meaning
$(A/F)_s$	Stoichiometric air-to-fuel ratio
C_{tot}	Total capacitance of the DC bus
J_d	Moment of inertia of the drive shaft
J_{genset}	Moment of inertia of the GENSET
λ	Air-to-fuel equivalence ratio
\dot{m}_{ci}	Cylinder-in mass flow
M_{ig}	Indicated gross torque
m_{veh}	Vehicle mass
n_{cyl}	Number of cylinders
η_{ig}	Indicated gross efficiency
$P_{max,nom}$	Nominal maximum ICE power
q_{HV}	Heating value of fuel
r_c	Compression ratio
r_w	Wheel radius
τ_{GEN}	Generator time constant
τ_{TM}	Traction motor time constant
T_{com}	Communication cycle time between PCM and CUs
u_f	Fuel-injection control signal
u_{wg}	Wastegate control signal
U	DC bus voltage
v_{veh}	Vehicle speed
ω_{ice}	Engine speed
ω_d	Drive shaft speed
γ_{cyl}	Effective specific heat capacity ratio
γ	Driving resistance loss factor

CONTROL RELATED NOTATION

Notation	Meaning
α_{ap}	Accelerator pedal position [0..1]
β	Proportion of produced ICE torque allowed for shaft acceleration
i_e	Effective gear ratio
K_p, K_i	Proportional and integral controller gains
$k_{p,LIG}$	Proportional gain for Low Idle Governor
$k_{p,red}$	Proportional reduction factor
M_{clip}	Torque clipped by the maximum traction power limit
M_{gen}	Torque generated by the GEN
M_{ice}	Torque generated by the ICE
M_{tm}	Torque generated by the TM
\hat{M}_{loss}	Estimation of braking torque due to engine losses

1

Introduction

In a diesel-electric powertrain, the wheels are mechanically decoupled from the internal combustion engine (ICE). In this powertrain configuration the engine speed is a free variable and can be independently chosen regardless of the vehicle speed, which enables both performance improvements and potential fuel consumption reductions, as well as bigger freedom regarding the physical placement of the ICE in the vehicle.

BAE Systems Hägglunds AB designs and delivers diesel-electric powertrains to be integrated into customer's vehicles. The traditional control approach in these powertrains is to let the driver control the electric traction motor (TM), while the generator (GEN) controls the DC voltage and the ICE achieves engine speed control. In other words, power is *pulled* through the powertrain. However, if the TM consumes more power than the ICE can produce, due to for example reduced ICE performance, the ICE will start to decelerate and ultimately stall. The established way of handling this problem makes full utilization of the available engine power difficult or even impossible.

In order to circumvent this drawback, an idea of a new control approach has emerged, in which the control structure is inverted; instead of letting the driver control the power consuming side of the powertrain (the TM), the driver controls the power producing side (the ICE). With this strategy, power is *pushed* through the powertrain instead. In this thesis, the characteristics of this new approach are investigated.

1.1 Motivation

The problem with utilizing the full ICE power leads to a need to oversize the engine. An improved control strategy without this problem would allow for a smaller engine to be used, coming with advantages such as lower purchasing

costs, relived physical space requirements and lower vehicle weight.

1.2 Purpose

The main purpose of the thesis is to investigate the characteristics of the new, prospective control strategy. There is also a secondary purpose to compile a plant model of the powertrain with a more sophisticated model for the ICE incorporating the turbocharger dynamics.

1.3 Problem formulation

These problem statements reference the established and the proposed control strategies. Descriptions of these strategies are found in Chapter 2.

- How can a control system working according to the proposed strategy be realized?
- Which advantages and disadvantages does the proposed control strategy posses?
- Are there other control strategies that are worth considering for this application?

1.4 Delimitations

Throughout the thesis, certain delimitations are made.

- There has been no possibility to test the developed control strategy on the physical vehicle, as this equipment has not been available. Thus, validation of proper functioning of the final control strategy is limited to simulations.
- In the developed powertrain model, focus is concentrated on the components from the ICE to the TM. Components downstream from the TM (final drive, vehicle dynamics, etc.) are disregarded or greatly simplified.
- Adding an energy storage to the system is not considered an option.
- Only vehicle movements in the forward direction are regarded.
- The maximum torque curves of the electric machines are not regarded and thus, they are assumed to be infinitely strong. This is motivated with the ICE typically being the power limiting component.
- The thesis is limited to only study the drivability and traction performance aspects, as opposed to for example the fuel consumption aspect.

1.5 Requirements

The main requirements on the developed control strategy are listed below.

- **Maximum utilization of available engine power**

Maximum available engine power should be delivered whenever the power demand is equal to or greater than the same. This implies that the control strategy has to be robust enough to handle limitations in engine performance (i.e. the engine not being able to deliver the full nominal power) due to for example high-altitude driving or engine malfunctioning.

- **Ability to handle high-priority external loads**

The control strategy must be able to handle the presence of high-priority external loads, which should take precedence over propulsion whenever they occur. To describe the desired behavior when this happens, two example cases are given. In these examples, $P_{max,nom}$ stands for nominal maximum ICE power and $P_{max,curr}$ for the maximum power *currently* available from the ICE. That is, a reduction from nominal engine power might be present.

- Assume full ICE performance (i.e. $P_{max,curr} = P_{max,nom}$) and that 50% of $P_{max,nom}$ is being used for propulsion. Suddenly, an auxiliary load also requiring 50% of $P_{max,nom}$ appears. The ICE should then deliver 100% of $P_{max,nom}$, of which 50% goes to propulsion and 50% to the auxiliary load.
- Now assume the same scenario except the ICE performance is reduced by 30% (i.e. $P_{max,curr} = 0.7P_{max,nom}$). The ICE should then deliver the full $P_{max,curr} = 0.7P_{max,nom}$, of which $0.5P_{max,nom}$ goes to the auxiliary load and $0.2P_{max,nom}$ to propulsion. In other words, the auxiliary load is prioritized while traction is reduced.

1.6 Outline

The thesis is divided into the following chapters, except this introductory chapter.

- **Chapter 2 - The Diesel-Electric Powertrain**

Gives a system description of the studied powertrain, together with descriptions of the established and proposed control strategies.

- **Chapter 3 - Approach**

Describes how the problem is approached and the drive cycles used when evaluating the control strategies.

- **Chapter 4 - Related Research**

Presents the outcome of the study of related research.

- **Chapter 5 - Modeling**

Explains and motivates the developed powertrain model.

- **Chapter 6 - Control Strategy Development**
Presents the findings from the control strategy development phase.
- **Chapter 7 - Results**
Presents the final control strategy together with simulation results with this strategy implemented.
- **Chapter 8 - Discussion**
The results and insights from the work are discussed.
- **Chapter 9 - Conclusions & Future Work**
The conclusions drawn from the work are summarized and suggestions for future work are given.

2

The Diesel-Electric Powertrain

The diesel-electric powertrains from BAE System Hägglunds AB are typically used in low speed, high torque applications. Two examples of these applications are reachstackers and aircraft tow trucks, as shown in Figure 2.1. In a conventional diesel powertrain for these applications, mechanical power from the ICE is transmitted through shafts and other mechanical components to the driveshaft, see Figure 2.2. In a diesel-electric powertrain on the other hand, the mechanical power from the ICE is first converted into electrical power in a generator and then transmitted through cables to an electric traction motor. This motor is, in turn, mechanically connected to the driveshaft, see Figure 2.3.



Figure 2.1: Typical applications of BAE Systems Hägglunds diesel-electric powertrains: (a) reachstackers and (b) aircraft tow trucks (NOTE: these pictures are included after approval from their respective originators).

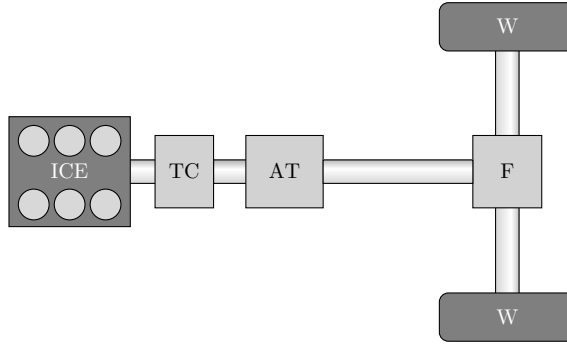


Figure 2.2: Simplified schematic of a conventional diesel powertrain. The power is transmitted from the internal combustion engine (ICE) to the wheels (W) through shafts and other mechanical components (TC = torque converter, AT = automatic transmission, F = final drive).

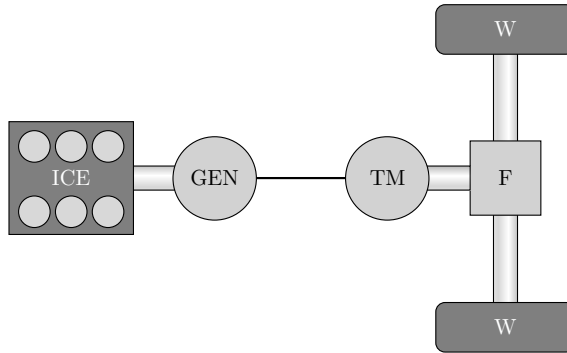


Figure 2.3: Simplified schematic of a diesel-electric powertrain. Mechanical power from the internal combustion engine is converted into electric power in a generator (GEN). It is then transmitted through cables to an electric traction motor (TM) which is mechanically connected to the wheels (W), usually through a final drive (F).

In a diesel-electric powertrain configuration, the wheels are mechanically decoupled from the ICE, which comes with several advantages.

- Another degree of freedom is introduced when the ICE speed can be freely chosen regardless of the vehicle speed.
- Bigger freedom regarding the physical placement of the ICE, since routing of electrical cables usually is a less complex concern compared to connecting the components mechanically.
- The electric traction motor allows for maximum torque output from stand-still.

These advantages typically come at a cost of reduced driveline efficiency since the required energy conversions introduce losses. Another disadvantage with a diesel-electric powertrain is of economical nature; the components of the powertrain are usually more expensive compared to the conventional counterparts.

2.1 System description

In Figure 2.3, a greatly simplified schematic of a general diesel-electric powertrain was presented. In this section, a more detailed description of the studied powertrain is given.

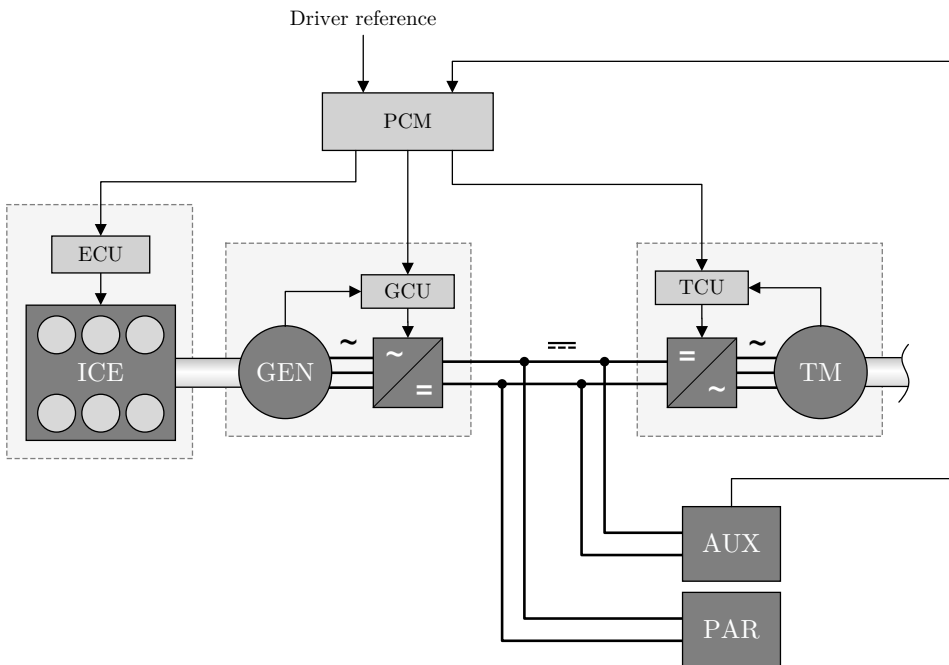


Figure 2.4: A more detailed schematic of the studied powertrain, including power electronics, controllers, control signals and also auxiliary and parasitic loads connected to the DC bus. The components downstream from the traction motor (TM) are omitted. Thick lines represent electric power transmission and narrow lines control and/or measurement signals. Dark grey blocks represent high-power components and light grey blocks control units. Dashed, light gray boxes highlight coherent subsystems.

Figure 2.4 shows a schematic of the studied powertrain. Below, brief descriptions of the components are given.

- **Internal combustion engine (ICE) with engine control unit (ECU)**
A diesel engine produces crankshaft torque and is controlled with its ECU.

These two components are delivered together as a coherent subsystem. The engine considered in this thesis is a turbocharged Cummins™ 6-cylinder 6.7-litre engine with fixed-geometry turbine and wastegate for boost control. The maximum ICE power is 205 kW.

- **Generator (GEN), inverter and generator control unit (GCU)**

A generator converts the mechanical power from the ICE to 3-phase AC electrical power, which is then converted to DC using an inverter. The two components are controlled with a generator control unit. These components are working together as a coherent subsystem.

- **DC bus**

The DC power transmission between the inverters is referred to as the *DC bus*. The nominal voltage in this bus is typically around 750 V.

- **Traction motor (TM), inverter and traction control unit (TCU)**

The DC power in the DC bus is inverted to AC and then fed to the traction motor. The two components are controlled via a traction control unit, and together they form a subsystem.

- **Auxiliary load (AUX)**

The main external load, referred to as the AUX load, is typically a high-power hydraulic demand in the reachstacker case. This load consumes power from the DC bus and its magnitude is known to the PCM. The maximum AUX load is 100 kW.

- **Parasitic load (PAR)**

Similar to the AUX load, a parasitic load with a maximum magnitude of 20 kW may consume power from the DC bus. The difference from the AUX load is that the magnitude of the PAR load is *not known* to the PCM.

- **Powertrain control module (PCM)**

The powertrain control module is the superior control node for the whole powertrain. It uses driver input and measured signals to set out appropriate reference signals to the ECU, GCU and TCU. The control strategy logic is implemented in this unit.

2.2 Control

As shown in Figure 2.4, the ICE and the electric machines all have individual control units. These control units can operate in different control modes. Descriptions of these modes are presented in this section.

2.2.1 ECU

The ECU follows the SAE J1939 standard [1]. In this thesis, two control modes are of interest.

- *Torque control*: given a torque reference, the ECU calculates the corresponding amount of fuel needed. As stated in the standard, the reference torque is interpreted as an indicated torque (as opposed to a braking torque), implying that no friction and pump loss compensation is done.
- *Speed control*: given a speed reference, the ECU controls the speed of the engine.

2.2.2 GCU & TCU

The GCU and TCU have three different operating modes.

- *Torque control*: given a torque reference, the control unit controls the shaft torque of the electric machine
- *Speed control*: given a speed reference, the control unit controls the shaft speed of the electric machine
- *Voltage control*: given a reference voltage, the control unit controls the voltage in the DC bus

Block diagrams of these control modes are shown in Figure 2.5.

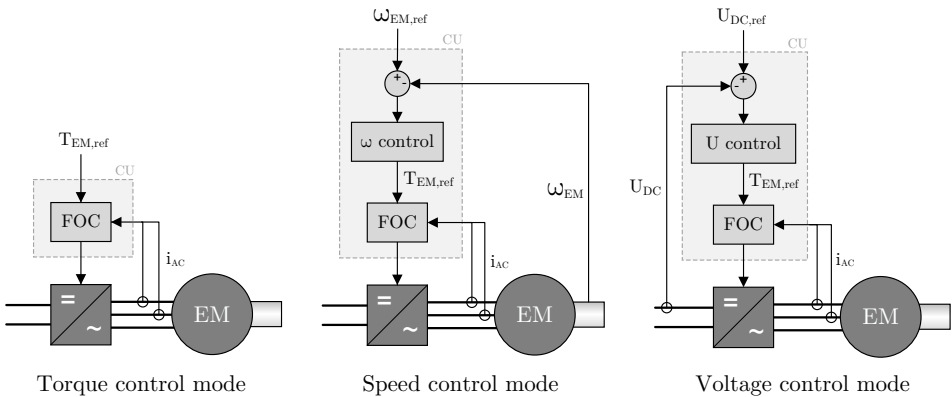


Figure 2.5: Control modes of the inverters. The electric machine (EM) torque is controlled by field-oriented control (FOC), which is not explained further in this thesis. More information regarding this control principle can be found in [11] and [19]. The dashed grey rectangles represent the control units (CU).

Controller parametrization

The control parameters in the GCU and TCU controllers can be individually set at runtime through CAN messages.

LimitRegenPower & LimitMotoringPower

It is possible to set limits on how much regenerative and motoring power the GCU and TCU should allow the electric machines to produce through CAN messages. These messages are called *LimitRegenPower* and *LimitMotoringPower*, respectively.

2.2.3 Control limitations due to subsystem boundaries

In an ideal, academic context any control law can be applied anywhere in the system. However, in the applied case studied in this thesis, this is not possible due to how subsystems are delivered as coherent components from external suppliers. With limited communication interfaces between units and predetermined control logic in the delivered controllers, the design freedom is greatly reduced. These limitations could theoretically be circumvented by developing the subsystem control units (ECU, GCU, TCU) completely from scratch, but this is not practically feasible due to the immense cost this would imply. For this reason, the use of standard components is strived for in the highest possible extent.

2.3 Communication

The PCM communicates with the other control units via a controller area network (CAN) bus. The communication is not instantaneous but occurs with a nominal maximum cycle time between messages. Prioritization mechanisms then ensure that the nominal maximum cycle time is not exceeded.

The nominal cycle time is set to 10 ms for all messages in this thesis.

2.4 Established control strategy (CS1)

With the established control strategy, referred to as control strategy 1 (CS1), the main idea is that the driver is in control of the traction torque, while the generator takes care of voltage control and the engine controls the engine speed. Both the voltage control and speed control are realized on subcomponent level in the GCU and ECU, respectively. A block diagram showing this strategy is presented in Figure 2.6.

2.4.1 Torque reduction

The *nominal* maximum power of the ICE is known to the PCM. Hence, the traction power can be saturated to not exceed this value. However, if the ICE has reduced performance due to for example high altitude driving conditions or engine malfunction, the *actual* maximum power is lower. This actual value is unknown to the PCM. If the TM consumes more power than the ICE can produce, the engine will decelerate and ultimately stall.

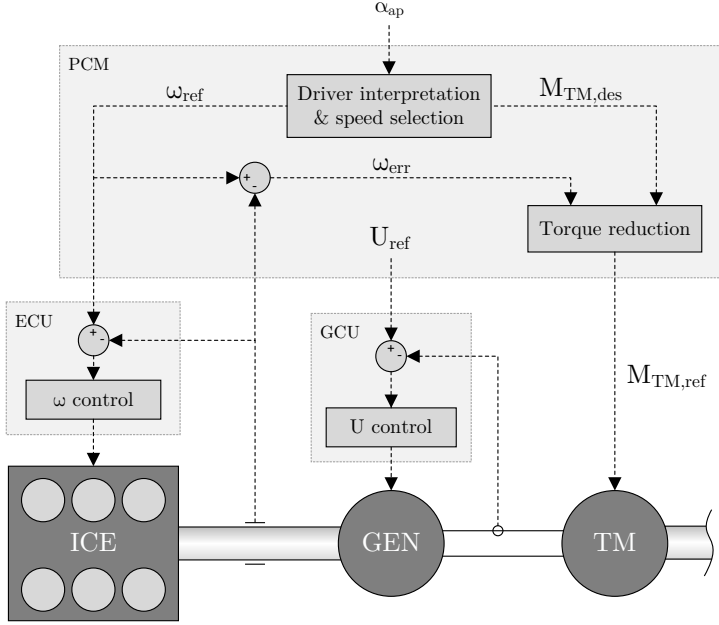


Figure 2.6: Simplified block diagram of the established control strategy (CS1) where power electronics and FOC blocks have been omitted for simplicity.

To circumvent this problem, a traction torque reduction is used. The TM torque is reduced proportionally to the engine speed error ω_{err} with a deadband ω_{db} . This technique can be mathematically described with

$$M_{TM,ref} = M_{TM,des} - k_{p,red}\omega_{red} \quad (2.1)$$

$$\omega_{red} = \begin{cases} \omega_{err} - \omega_{db}, & \text{if } \omega_{err} - \omega_{db} > 0 \\ 0, & \text{otherwise} \end{cases} \quad (2.2)$$

where $M_{TM,ref}$ is the actual torque reference to the TM, $M_{TM,des}$ the torque desired by the driver, $\omega_{err} = \omega_{ref} - \omega$ the engine speed error and ω_{db} the deadband. In this way, the TM will decrease its torque until a stationary operating point is reached, thereby preventing the engine to stall.

2.4.2 Pull analogy

When the driver demands torque from the TM, the voltage in the DC bus will drop as a consequence of the increased power consumption. To counteract this, the GEN, being the voltage controlling unit, will start to load the engine shaft and feed power into the bus. This will decelerate the shaft and thus increase the speed error, which will cause the ECU to increase the produced ICE torque

in order to maintain the speed. In summary, the driver initiates power output from the consuming side of the powertrain and gets the components upstream to produce the corresponding power. Hence, this strategy can be seen as a *pull* strategy. In Figure 2.7, this principle is visualized.

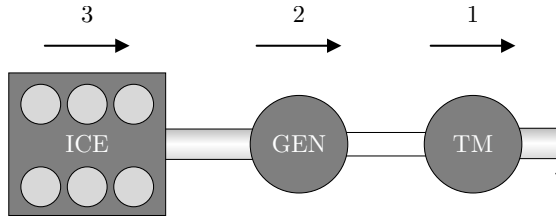


Figure 2.7: Schematic demonstrating the pull principle. The driver initiates power consumption in the TM (1) causing the voltage to drop. The GEN responds to the decreasing voltage by loading the engine shaft and feeding power into the DC bus (2) causing the shaft to decelerate. Finally, the ICE reacts to the declining shaft speed by producing the required power (3).

2.4.3 Maximum power utilization problem

The main problem with CS1 is utilizing the full power available from the engine. As described in Section 2.4.1, the maximum engine power might be time-varying due to for example engine malfunctioning or high-altitude driving conditions and is therefore unknown to the PCM. When the power consumed by the TM exceeds the maximum power currently available from the ICE, the engine will decelerate, the speed error increase and the torque reduction eventually kick in. Ultimately, the powertrain will reach a stationary operating point when the torque reduction is of sufficient size. When this occurs, however, the engine speed will settle with a constant error since the reduction is purely proportional (compare with a proportional controller). A lower engine speed implies that an even lower maximum power will be available from the ICE due the shape of its maximum power curve (typically increasing maximum power with increasing engine speed). Hence, even if the driver requests full power only part of it will be produced.

This problem is demonstrated in Figure 2.8. In (a) the engine has the full nominal power available (205 kW) and it is seen that the traction power reaches up to and settles at the desired level. In (b) however, engine performance is reduced by 30%, leading to a maximum power of 143.5 kW. In this case, the traction power settles at a lower-than-available level (approximately 117 kW) and the engine speed establishes a significant constant error. So, even though the driver requests maximum available power only approximately 82% of it is delivered.

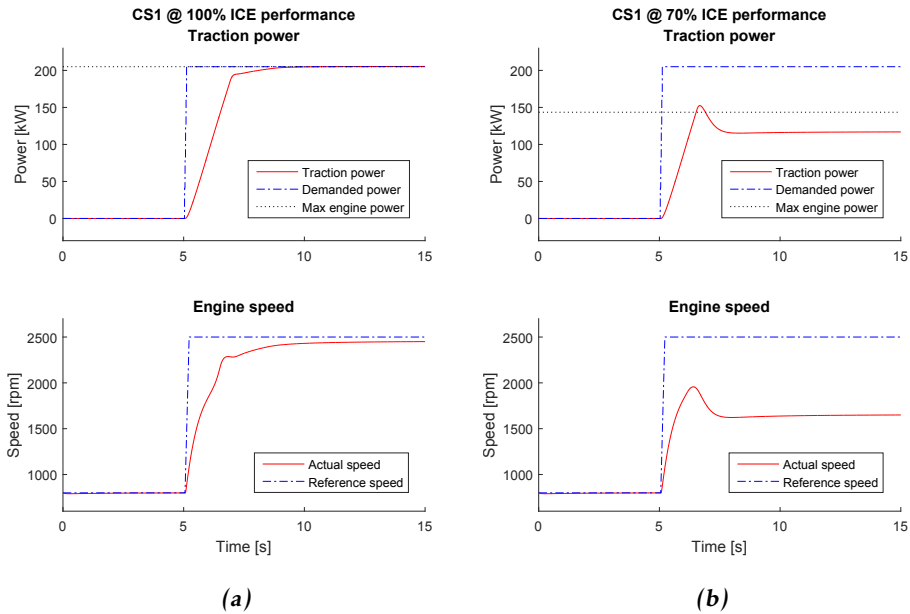


Figure 2.8: The main problem with CS1 demonstrated using a step in demanded power from 0% to 100%. In (a) the engine has the full nominal power available (205 kW), while in (b) the maximum power is reduced by 30% to 143.5 kW.

2.5 Proposed control strategy (CS2)

In order to circumvent the problem with CS1, a new control approach is proposed. The principal idea is to invert the control structure; instead of having the driver control the traction motor (i.e. the power consuming part of the powertrain), the driver controls the engine (i.e. the power producing part). Meanwhile, the GEN takes care of engine speed control and the TM realizes voltage control. A block diagram of the proposed control strategy is presented in Figure 2.9.

2.5.1 Push analogy

When the driver initiates torque generation from the ICE, the shaft will start to accelerate. The GEN, being the speed controlling component, will counteract this acceleration by loading the shaft with a braking torque in order to keep the speed at the desired level. This will in turn feed power into the DC bus and cause the voltage to increase. The TM will therefore start to consume power by generating torque in order to keep the voltage at the reference level, and traction is achieved consequently. Hence, CS2 can be seen working according to a *push* principle. This concept is visualized in Figure 2.10.

An interesting remark is that the proposed control strategy is analogous to the

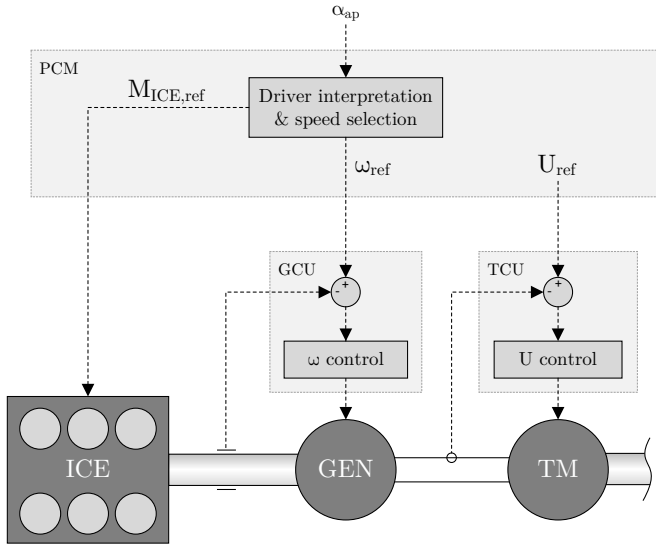


Figure 2.9: Block diagram of the proposed control strategy (CS2).

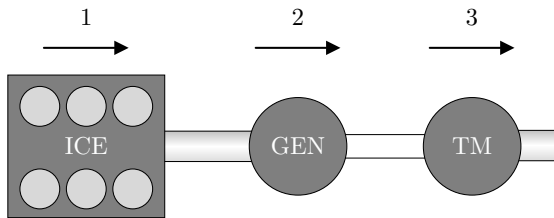


Figure 2.10: Schematic demonstrating the push principle. The driver controls the ICE to produce power (1) causing the shaft to accelerate. The GEN responds to this acceleration by loading the shaft and feeding power into the DC bus (2), which causes the voltage to increase. Finally, the TM counteracts the increasing voltage by consuming power from the bus and thus generating traction (3).

way a conventional diesel powertrain is controlled; the driver has control over the power producer in the powertrain (the ICE) instead of the power consumer (the wheels). By initiating torque generation from the engine, traction is obtained consequently.

3

Approach

This chapter presents the approach and working process of the thesis. The work is divided into a number of different phases, which are explained below. A visual representation of the process is shown in Fig 3.1.

1. Literature study

A study of related research is conducted in order to find out what work has been done in the field, state-of-the-art technologies, and so forth.

2. Modeling

In order to have a plant model to develop and evaluate the control strategies on, such a model is compiled. The model is implemented in MATLAB™/Simulink™.

One major component that have been simplified in previous models is the ICE. Thus, a new model for this component is implemented in order to catch dynamic phenomena such as the turbocharger dynamics. In [15] a validated model for a similar diesel-electric powertrain is developed and presented. In [4] an optimal-control oriented MATLAB™ implementation of this model is provided under the name *LiU-D-El* which is implemented during the modeling phase.

3. Implementation of established strategy

A control strategy working according to the established approach is implemented in order to reproduce the problem of interest.

4. Control strategy development

Starting with the proposed control approach, a development loop is iterated. After implementing the initial idea, the performance and characteristics of the approach are evaluated and a new, refined idea is generated. The procedure is then repeated.

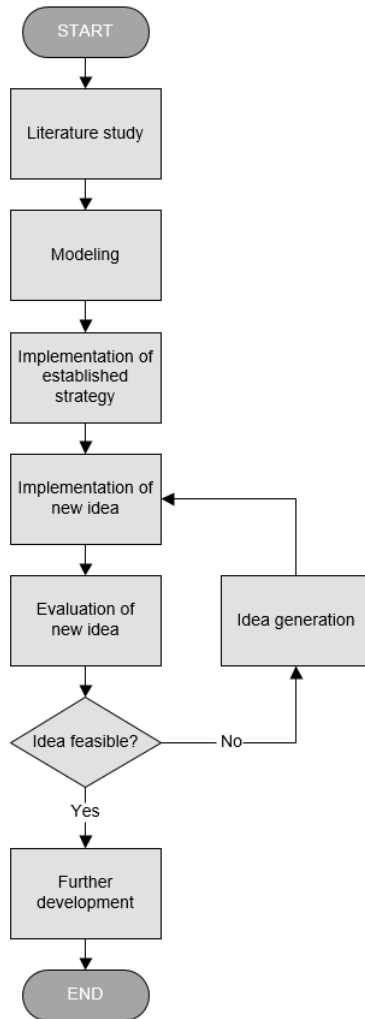


Figure 3.1: A block diagram presenting the work process of the thesis.

5. Further development

When a promising control approach is found, the development loop is exited and the final idea further refined.

3.1 Drive cycles

The control strategies are developed and evaluated using two different drive cycles: a fictive one and a real one.

3.1.1 Fictive drive cycle

In order to be able to clearly analyze control strategy performance during a set of distinct transients, a fictive drive cycle is formed. This drive cycle is presented in Figure 3.2. The main idea is the following:

- The accelerator pedal performs steps to 10%, 50% and 100% of nominal engine power (205 kW), and then steps down.
- The auxiliary load steps up to 100% of its nominal max load (100 kW) and then down while the accelerator pedal requests full power.
- The parasite load steps up to 100% of its nominal max load (20 kW) and then down while the accelerator pedal requests full power.

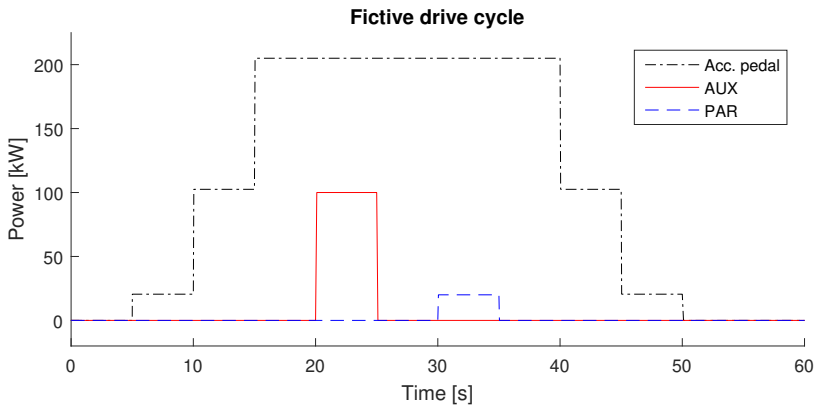


Figure 3.2: Fictive drive cycle.

3.1.2 Real drive cycle

The second drive cycle is from a real driving scenario. The accelerator pedal and AUX signals have been recorded for a longer period of time during real driving, and a 273 second excerpt from these recordings are used as a more realistic driving mission. This drive cycle is shown in Figure 3.3.

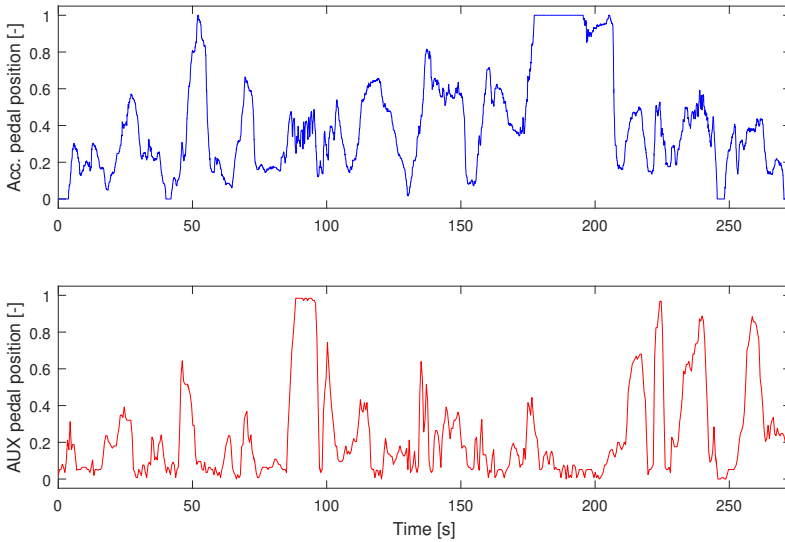


Figure 3.3: Real drive cycle.

4

Related Research

4.1 Control

A diesel-electric powertrain is not a hybrid powertrain since it uses only one source of energy. Though, its layout is similar to the one of a series hybrid electric powertrain. The main difference between the two is that the latter, in addition to chemical fuel storage, also has an electric energy storage which can supply power to the electric bus. Thus, control of a diesel-electric powertrain should be similar to control of a series hybrid electric powertrain when the electric energy storage is empty and/or non-utilizable. This mode of operation is described as “Engine/Generator-Alone Traction Mode” in [5] and [10]. However, this operating mode is seemingly not the preferred operating mode in such a powertrain, which is obvious in [10] where the propulsion system of a series hybrid electric vehicle (SHEV) is described as “an electric motor with batteries that can be charged through a generator driven by an ICE”. Hence, the primary function of the engine-generator set is not powering the traction motors directly.

Seemingly, there is a relatively scarce amount of research that has been conducted regarding control of purely diesel-electric powertrains when compared to the field of SHEVs. Thus, it is of interest to investigate how SHEVs are controlled in the operating mode described above. However, the majority of the publications found regarding control of SHEVs cover control strategies for energy management in the vehicle, for example how to control the state-of-charge (SOC) in the battery pack, which is a completely different problem (Barsali et al. presents this control problem in a good way in [2]). This further speaks for the main purpose of the engine-generator set (GENSET) being charging the batteries as stated in [10], rather than directly providing power to the traction motors.

Two applications for diesel-electric powertrains are railroad locomotives and marine ships [12], [3]. In the marine case, diesel-electric propulsion started to

gain popularity in the 1980s when advances in switching power electronic technology made new ways of variable speed control of electric motors possible [8]. Since then, a considerable amount of research work has been carried out about electric propulsion in marine vessels. In [7], Geertsma et al. presents a thorough summary of different marine propulsion architectures, including the features and layout of the electrical propulsion architecture. From this summary, it is obvious that a typical diesel-electric powertrain in a marine application resembles the powertrain studied in this thesis, but also has several differences. One important difference is the power distribution system: in marine applications, the electrical power is usually distributed on a fixed-frequency AC grid while the studied powertrain has a DC bus. However, Hansen and Wendt [8] state that DC transmission on marine vessels is a promising new solution.

The summary of marine electrical propulsion in Geertsma et al. [7] shows that the common way to control a marine diesel-electric powertrain is to control the speed of the engines to provide the desired grid frequency, control the generator to maintain a certain voltage and then control the electric motors to keep up a desired propeller speed. Thus, this resembles a pull strategy similar to the established strategy for the studied powertrain. There are two main differences though.

- In the marine case, the demand signal from the driver is a speed reference, while it is a torque reference in the studied case. However, research has shown that torque/power control of the shaft might be advantageous [18]. If torque control was used in such a powertrain, its control strategy would be principally very similar to the established strategy in the studied powertrain.
- The engine speed in the marine application has to be fixed in order to produce AC power with the appropriate frequency for the AC grid. In the studied application, where a DC grid is used, the engine speed can be freely chosen since the provided frequency is not of importance.

A particular interest during the literature study has been whether the proposed push principle has been previously investigated or not. However, powertrain control according to this approach has not been encountered during the study.

4.2 Modeling

Since the secondary purpose of the thesis is to compile a powertrain model with a more sophisticated ICE model incorporating turbocharger dynamics, the importance of such an incorporation has been investigated. In [13], Nezhadali et al. conclude that omitting the turbocharger dynamics in models for transient time and fuel consumption calculations can incur underestimates of both time and consumption of over 60% in transients.

There has been extensive research done within the field of modeling of turbocharged internal combustion engines. Eriksson and Nielsen thoroughly presents

methodology for both modeling and control of engines and drivelines in [6], using the work from over 300 relevant publications and textbooks.

In [20], Eriksson and Wahlström presents a full mean-value model of a turbocharged diesel engine with variable-geometry turbine and exhaust gas recirculation, and also provide a Simulink™ implementation of the model. Even though the studied powertrain has an engine with fixed-geometry turbocharger and wastegate for boost control, big parts of the work from Eriksson and Wahlström might be relevant in this case, allowing for model re-usage and a potential decrease in the amount of model development effort needed.

Regarding modeling of diesel-electric powertrains specifically, Sivertsson and Eriksson present a validated model of a diesel-electric powertrain in [15]. The model is developed with focus on optimal control and covers the engine-generator set only, but might surely be useful throughout this thesis. For example, this model describes the same turbocharger configuration as in the studied case (fixed-geometry turbine with wastegate), which could be a better basis than the model in [20] for this thesis.

The same Sivertsson and Eriksson also investigate optimal transient control trajectories in diesel-electric systems in [16] and [17]. The conclusions from these publications might be used in controller design to tackle the problem of how to optimally move the operating point of the diesel engine between different power levels.

Regarding modeling of diesel-electric powertrains in general, Hansen et al. presents a mathematical model of such a powertrain in [9]. The modeled powertrain has an AC distribution grid (as most marine vessels with diesel-electric propulsion do) and thus, it is principally different from the studied powertrain. However, even though the model itself might be irrelevant, modeling and control concepts used in the work is of interest for this thesis.

5

Modeling

In this chapter, the developed powertrain model is presented. The model is implemented in MATLAB™/Simulink™.

5.1 Internal combustion engine

As stated in Chapter 3, the diesel-electric powertrain model developed in [15] is implemented to catch dynamic phenomena of the engine. There are two different engine models provided, MVEM₀ and MVEM₂. MVEM₀ is modeled to get the efficiency characteristics of the specific engine studied in the article, while MVEM₂ represents a more generic engine. In this thesis, MVEM₂ has been chosen to make the developed model usable in a more general context.

The model is provided as a MATLAB™ function, and is therefore implemented using a MATLAB™ function block in Simulink™. The model is implemented in its original, non-modified form. However, certain customizations have been necessary to get the model to work properly in this context, which are explained in the following sections.

The Simulink™ implementation of the ICE model is shown in Figure 5.1.

5.1.1 States and control inputs

The model comprises the engine, the shaft, the generator and the power electronics. It has four states:

- intake manifold pressure
- exhaust manifold pressure
- turbocharger speed

- engine speed

and three control signals:

- injected fuel mass
- wastegate position
- generator power

In this thesis, both the shaft and the generator are modeled individually. Thus, the engine speed state is not used and the generator power control signal is set to zero.

5.1.2 Internal signals and outputs

From the original model, there are five output signals: derivatives of the four states and a struct c with additional quantities. Since the main aspect of interest in this context is the torque generation, another output signal M_{ice} with the engine torque is added. Also, an output signal \dot{m}_{ci} with the cylinder-in mass flow is added since it is needed both for lambda calculation and in the ECU model.

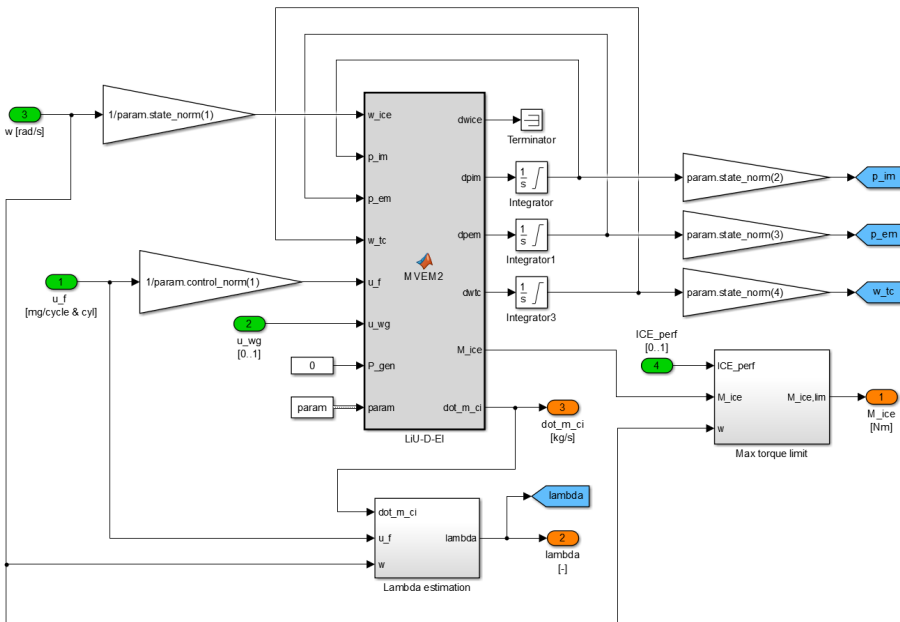


Figure 5.1: Simulink™ implementation of the LiU-D-EI model.

5.1.3 State and control signal normalization

The provided model works with normalized values for both the states and the control signals. Thus, a normalizing/denormalizing layer has to be wrapped around the MATLAB™ function, making use of norm values which are all provided together with the model.

5.1.4 Maximum torque limit

The engine net torque M_{ice} is saturated using the maximum torque curve, ensuring the engine model does not generate a higher torque than physically possible.

5.2 ECU

As described in Section 2.2.1 the ECU control modes of interest in this thesis are torque control and speed control. These are implemented together with a *mode* signal in order to enable mode switching as desired.

5.2.1 Fuel feed-forward

From the torque request coming either directly from the PCM or from the ECU speed controller, the required fuel mass to be injected is calculated. An inversion of the engine torque model for the indicated gross torque M_{ig} as described in [15] is used, according to

$$M_{ig} = \frac{u_f n_{cyl} q_{HV} \eta_{ig}}{4\pi} \Rightarrow u_f = \frac{4\pi M_{ig}}{n_{cyl} q_{HV} \eta_{ig}} \quad (5.1)$$

where η_{ig} is calculated as

$$\eta_{ig} = \eta_{ig,t} \left(1 - \frac{1}{r_c^{\gamma_{cyl}-1}} \right) \quad (5.2)$$

and $\eta_{ig,t}$ as

$$\eta_{ig,t} = \eta_{ig,ch} + c_{u_f,1} \left(\frac{u_f}{\omega_{ice}} \right)^2 + c_{u_f,2} \frac{u_f}{\omega_{ice}} \quad (5.3)$$

The parameter data provided with the model are used for the parameters in the above expressions.

5.2.2 Smoke limiter

In diesel engines, the air-fuel equivalence ratio λ should not be allowed to fall below a certain level to prevent smoke (particulate matter) generation, as described in [6]. Thus, a smoke limiter is implemented to limit the amount of fuel injected depending on how much air is available for the combustion. The desired fuel

mass $u_{f,des}$ is limited with respect to the maximum allowed fuel mass $u_{f,max}$ according to

$$u_f = \min(u_{f,des}, u_{f,max}(\dot{m}_{ci}, \omega_{ice})) \quad (5.4)$$

In this equation, $u_{f,max}(\dot{m}_{ci}, \omega_{ice})$ is calculated as

$$u_{f,max}(\dot{m}_{ci}, \omega_{ice}) = \frac{4\pi\dot{m}_{ci}}{\omega_{ice}(A/F)_s\lambda_{min}n_{cyl}} \quad (5.5)$$

where \dot{m}_{ci} is the cylinder in mass flow, ω_{ice} the engine speed, $(A/F)_s$ the stoichiometric air-fuel ratio, λ_{min} the lower limit on λ and n_{cyl} the number of cylinders.

5.2.3 Low idle governor

According to the SAE J1939 standard [1], the ECU will not let the engine stall when controlled in torque control mode. When zero torque is requested, the engine will decelerate until the shaft speed drops below a certain low idle speed. At this point, a *low idle governor* (LIG) kicks in to prevent stalling. According to the standard, this governor can be implemented either using a maximum selection technique or a summation technique (described in figures SPN512_A and SPN512_B in the standard, respectively). In this thesis, the LIG is implemented using the maximum selection principle as a proportional controller, contributing with a torque request to the engine whenever the speed drops below the reference, according to

$$M_{ref} = \max(M_{ref,des}, k_{p,LIG}\omega_{err}) \quad (5.6)$$

where $k_{p,LIG}$ is the proportional gain of the LIG and ω_{err} is the speed error relative to the low idle speed.

5.2.4 Wastegate control

Control of the wastegate in turbocharged ICEs is a non-trivial matter. There are several possible principles that can be used, all having their advantages and disadvantages. In this thesis, where wastegate control is not the topic of interest, just a simple technique is enough in order to get sufficiently realistic engine behavior. Thus, a simplified control approach is used, where a PI controller actuates the wastegate to keep the air-fuel equivalence ratio λ at a specified setpoint. In this way, the wastegate will be open at stationary operating points (minimizing the back pressure and hence the fuel consumption) and closed during transients when more air is needed. This is considered to be a close-to-realistic behavior.

5.3 Genset shaft

The rotational speed of the genset shaft is modeled using Newton's second law for rotation, that is

$$M_{ice} - M_{gen} = J_{genset} \dot{\omega} \quad (5.7)$$

where M_{ice} is the engine torque, M_{gen} the generator torque, J_{genset} the moment of inertia of the GENSET and ω the rotational speed.

5.4 Generator, traction motor & inverters

The generator and the traction motor with their respective inverters are both modeled in the same way. They are simplified as first order systems with time constants of 10 ms, with transfer functions according to

$$M_{em} = \frac{1}{\tau_{em}s + 1} M_{ref} \quad (5.8)$$

where M_{em} is the actual torque produced by the EM, τ_{em} is the time constant and M_{ref} is the requested torque. This simplification is motivated with the fact that the dynamics of the EMs are significantly faster than the dynamics of the ICE, making the later the limiting component.

5.5 GCU/TCU

The generator and traction motor control units are very similar in functionality and are therefore modeled in the same manner. As described in Section 2.2.2, these control units can operate in either torque, speed or voltage control mode. These modes are all implemented together with a *mode* signal, making it possible to select operating mode from the PCM.

The output from the GCU/TCU is a reference torque to their respective electric machine models. Thus, the torque control mode is implemented simply as a direct forwarding from input reference torque to output reference torque. The speed and voltage controllers are then implemented as superior controllers outputting reference torque as control signals. Additionally, the *LimitRegenPower* and *LimitMotoringPower* signals described in Section 2.2.2 are also implemented.

The Simulink™ model of the GCU is presented in Figure 5.2 for clarity.

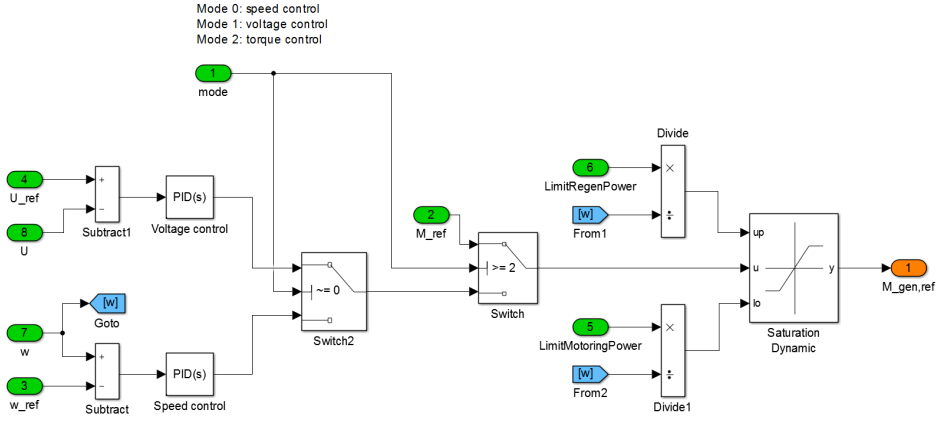


Figure 5.2: SimulinkTM model of the GCU. The TCU model is identical except sign conventions.

5.6 DC bus

The DC bus voltage is modeled using the relationship between current and voltage in a capacitive circuit

$$i(t) = C_{tot} \frac{dv(t)}{dt} \Rightarrow v(t) = \int \frac{1}{C_{tot}} i(t) dt \quad (5.9)$$

where $i(t)$ is the current, $v(t)$ the voltage and C_{tot} the total capacitance of the DC bus. Combining this expression with the power relation

$$P(t) = v(t) i(t) \Rightarrow i(t) = \frac{P(t)}{v(t)} \quad (5.10)$$

yields

$$v(t) = \int \frac{1}{C_{tot}} \frac{P(t)}{v(t)} dt \quad (5.11)$$

where $P(t)$ is the sum of all incoming (+) and outgoing (-) powers with signs. This gives the final expression

$$v(t) = \frac{1}{C_{tot}} \int \frac{P_{gen}(t) - P_{tm}(t) - P_{aux}(t) - P_{par}(t)}{v(t)} dt \quad (5.12)$$

5.7 Drive shaft & vehicle

The drive shaft speed is modeled in a similar way as the genset shaft, using Newton's second law for rotation. There are however two main differences.

5.7.1 Simplified loss assumption

The braking torque on the drive shaft comes from the driving resistance of the vehicle. A simplified loss assumption is made, yielding that the driving resistance (comprising air drag, rolling resistance, and so forth) is proportional to the vehicle speed and thus also to the drive shaft speed, that is

$$M_{br} = \gamma \omega_d \quad (5.13)$$

where M_{br} is the braking torque on the shaft, γ the loss factor and ω_d the drive shaft speed.

5.7.2 Reflected inertia

The mass of the vehicle reflects as moment of inertia on the drive shaft. The experienced moment of inertia that the TM effectively drives is

$$J_{exp} = \frac{J_{veh}}{i_d^2} + J_d \quad (5.14)$$

where

$$J_{veh} = m_{veh} r_w^2 \quad (5.15)$$

and i_d is the final drive gear ratio, J_d the drive shaft moment of inertia, m_{veh} the vehicle mass and r_w the wheel radius.

5.8 Bus communication

Communication between the PCM and the other powertrain control units (ECU, GCU and TCU) occurs with a certain cycle time as described in Section 2.3. This communication is simulated by introducing a communication layer with bus delays between the PCM and the actual powertrain. The bus delays are two back-to-back rate transition blocks, the first changing the sample rate to the specified cycle time and the second changing the rate back to the simulation sample rate. The effect of introducing these bus delays is shown in Figure 5.3.

The communication cycle time T_{com} is assumed to be 10 ms for all signals.

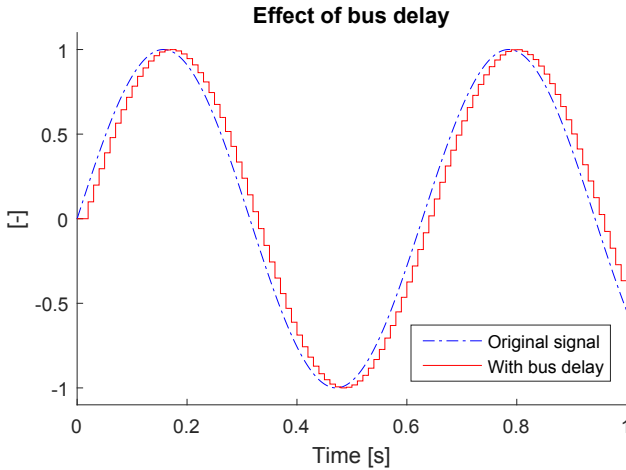


Figure 5.3: Effect of introducing a bus delay, demonstrated on a sine wave signal.

5.9 Model validation

Since no data from the real powertrain is available, validating the model against real measurements is not possible. Instead the model is validated by assessing the model behavior and confirming that it complies with the expected behavior. This validation is done both for the individual subsystems and for the complete powertrain with CS1 implemented.

5.9.1 ECU & ICE

Correct functioning of the ECU speed controller is validated by performing steps in both reference speed and braking torque (load). The results are shown in Figure 5.4. From these plots, it can be confirmed that this controller exhibits an expected behavior.

The ECU torque feed-forward is validated by performing steps in reference torque. The results are presented in Figure 5.5. Two phenomena are noticed:

- The actual torque never reaches the desired level, but settles with an offset. This can be explained with the engine friction and pump losses. As stated in the SAE J1939 standard [1], the torque request sent to the ECU is an indicated torque and not a braking torque. Thus, having this offset is the expected behavior. For example, requesting zero torque should imply a net braking torque on the shaft, which can be seen in the left plot.
- During the bigger step (the right plot), the effect of the turbo lag is obvious; when the step occurs, approximately 500 Nm is achieved immediately while the remaining torque is slowly ramped until the final value is reached,

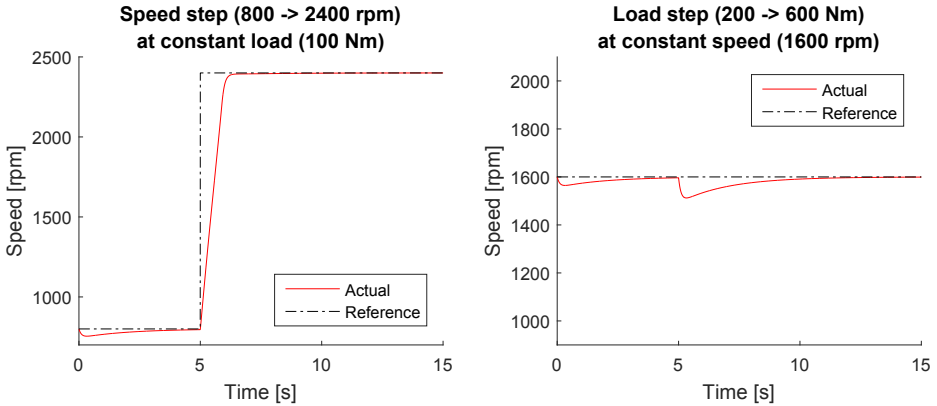


Figure 5.4: Validation of proper functioning of the ECU speed controller.

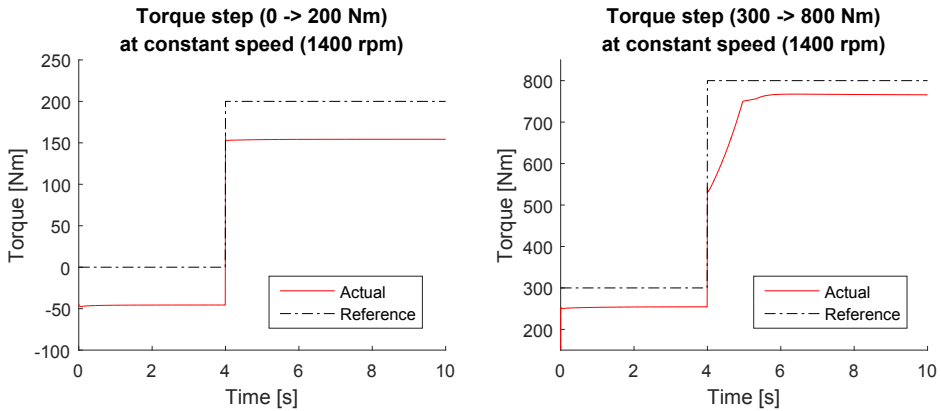


Figure 5.5: Torque step responses for the ICE.

taking a couple of seconds. This is due to an initial lack of air for the combustion, which is counteracted as the turbocharger speeds up and causes a higher intake manifold pressure.

5.9.2 GCU/TCU

Validation of the GCU and TCU is presented in this section. Since the GCU and TCU are modeled almost identically (the only difference is sign conventions), only validation for the GCU is presented since this is also applicable to the TCU.

In Figure 5.6, the correct functioning of the GCU speed controller is validated. As seen, the actual speed follows the reference curve in a satisfactory manner. However, it is worth recalling from the Delimitations section in Chapter 1 that the electric machines are modeled infinitely strong, so this high level of control performance is expected.

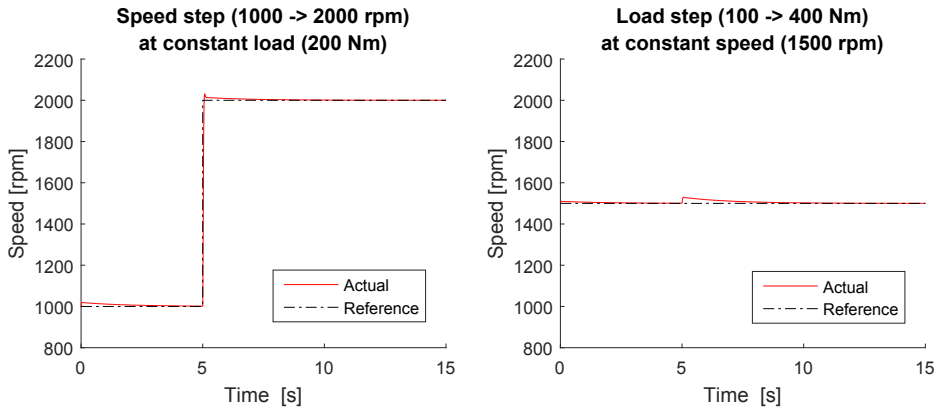


Figure 5.6: Validation of correct functioning of the GCU speed controller. In the left plot a step in reference speed is performed, and in the right plot a step in torque on the incoming shaft is performed.

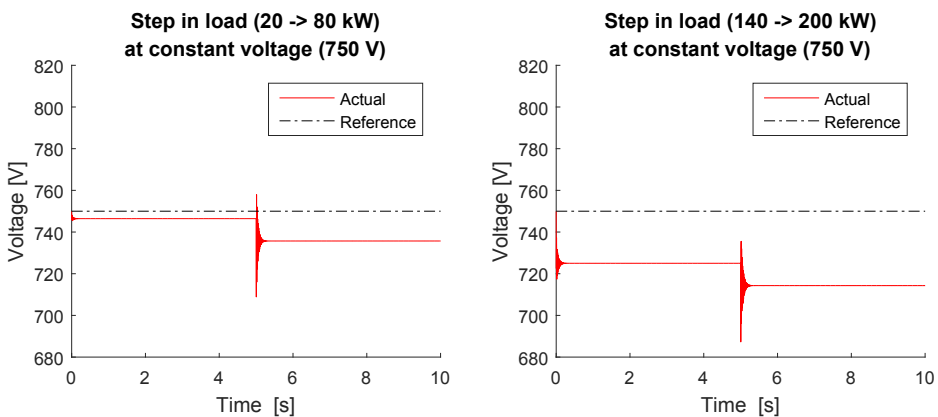


Figure 5.7: Validation of GCU voltage controllers.

Figure 5.7 shows validation plots for the GCU voltage controller. Two steps in load (i.e. power consumed from the DC bus) are performed and it is seen how the voltage drops consequently. Traditionally, voltage control has been achieved through proportional (P) control solely which is therefore implemented in the model. This causes the stationary control errors seen in the plots. Furthermore, high-frequency ringing is observed immediately after the steps. This is due to the quick dynamics of the DC bus posing a need for a high P gain in the controller in order to achieve adequate response.

5.9.3 Complete powertrain

Proper behavior of the complete powertrain model is validated by implementing CS1, performing a step in accelerator pedal position and assessing the response. The results from a simulation when a step from $\alpha_{ap} = 0$ to $\alpha_{ap} = 0.8$ is performed, are shown in Figure 5.8. It is observed how the traction power increases, causing a drop in both voltage and engine speed, which is the expected response with this control strategy. In this simulation, the GCU voltage controller realizes only proportional (P) control which explains the stationary error seen in these results.

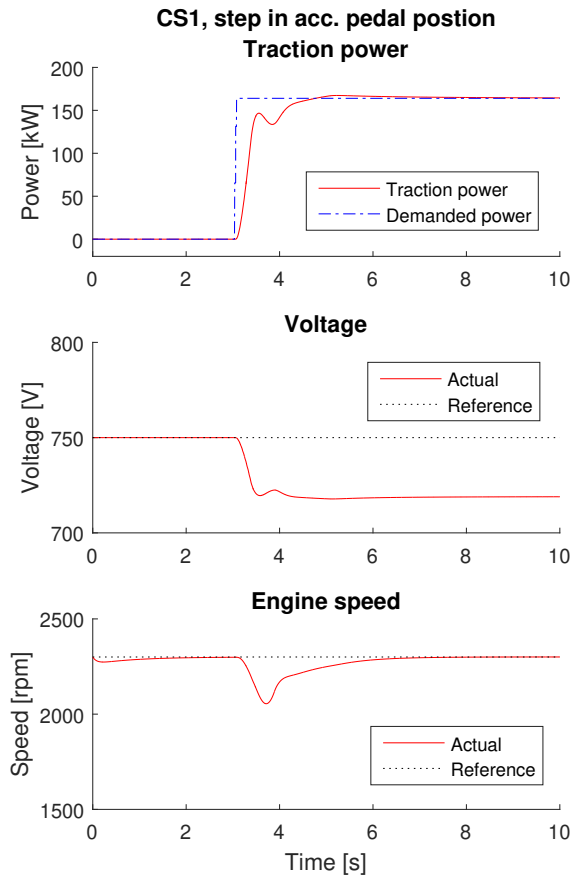


Figure 5.8: Simulation results when performing a step in accelerator pedal position from 0% to 80%.

6

Control Strategy Development

6.1 Proposed strategy (CS2)

The proposed control strategy as described in Chapter 2 is implemented in Simulink™. The approach exhibits two main problems.

6.1.1 Voltage control at standstill

In CS2, the TM is the voltage controlling actuator. Thus, it needs to be capable of both decreasing and increasing the voltage as necessary. A voltage decrease is achieved by generating accelerating torque on the drive shaft and hence consuming power from the DC bus. A voltage increase is achieved in the opposite way; the TM loads the drive shaft with a decelerating torque and regenerates power to the DC bus.

When the vehicle stands still (i.e. $v_{veh} = 0$) there is no kinetic energy available for the TM to use for increasing the DC voltage. Since the TM is the only voltage controlling unit, the voltage will drop if the ICE is not producing any power. This problem is confirmed in Figure 6.1.

6.1.2 Voltage control at no traction demand

As described in the previous section, the problem at standstill is to *increase* the voltage. When the driver requests no traction (i.e. the accelerator pedal position is zero, $\alpha_{ap} = 0$), another similar problem occurs. Requesting zero traction must of course imply zero traction torque and thus, the TM is not allowed to generate any torque. In this case, the problem is now to *decrease* the voltage. Since the TM is the only voltage controlling unit, there is no means of decreasing the voltage if this unit cannot.

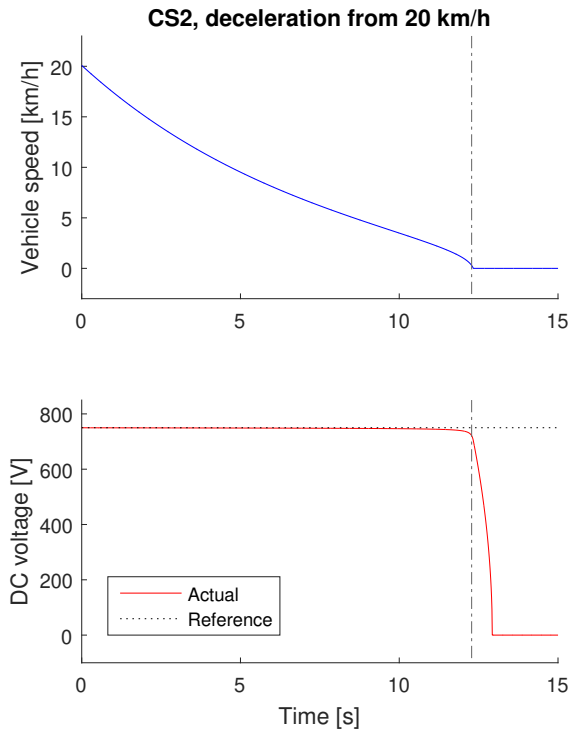


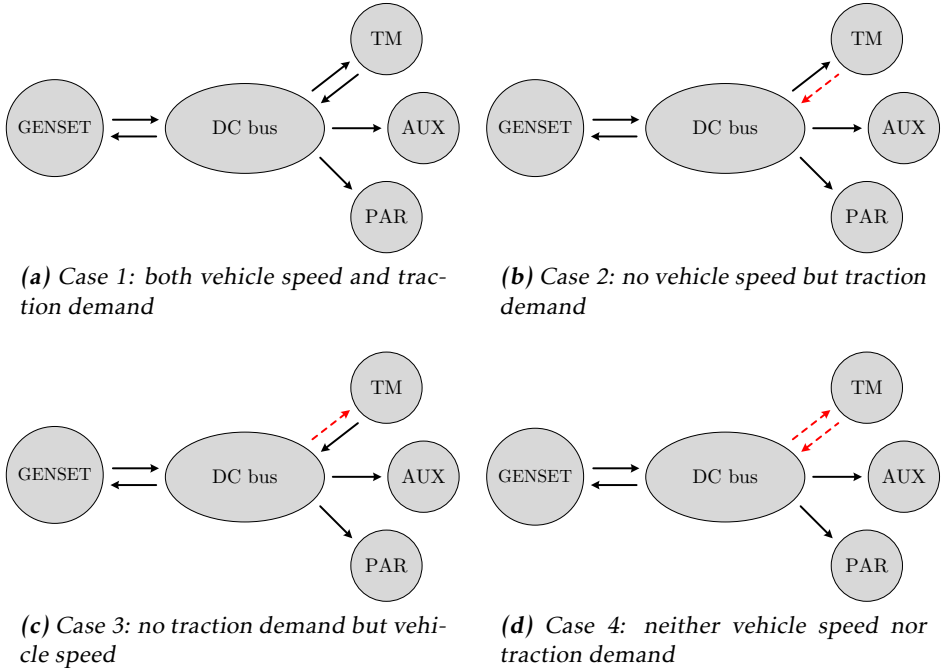
Figure 6.1: Standstill problem with CS2 demonstrated. The vehicle is decelerated from 20 km/h to 0 km/h simply by setting accelerator pedal position to 0%. While $v_{veh} > 0$, the TM is capable of keeping the voltage at the desired level. However, when the vehicle speed reaches 0 km/h (at around 12.3 s, marked with dash-dotted lines), the voltage drops as result of no kinetic energy being available for increasing the voltage.

6.1.3 Power path analysis

The discovered problems become obvious when analysing the power paths through the DC bus. Four different cases, as presented in Table 6.1, are of interest. In Figure 6.2, possible power paths for these cases are depicted. As shown, the AUX and PAR loads can only consume power from the DC bus, while the GENSET and TM can, under the right circumstances, both consume and produce power to the bus. There are, however, situations when the power directions of the TM are limited, which is the case in the problematic scenarios described above. In addition to these cases (no vehicle speed and no traction demand), there are two more possible scenarios: the "normal" driving case when there's both vehicle speed and traction demand, and the more extreme case when there's neither speed nor demand.

Table 6.1: Studied cases in the power path analysis.

Case	v_{veh}	α_{ap}
1	> 0	> 0
2	0	> 0
3	> 0	0
4	0	0

**Figure 6.2:** Analysis of power paths through the DC bus for different scenarios. Solid black arrows indicate possible paths for power transmission, and dashed red arrows indicate power path not possible in the specific scenario.**No vehicle speed (case 2 & 4)**

When there is no vehicle speed, the only unit able to increase the voltage (i.e. being able to provide power to the DC bus and hence, having arrows leading towards it) is the GENSET. Thus, this unit must take care of increasing the voltage in these cases.

No traction demand (case 3 & 4)

In the cases when there is no traction demand, there are three units able to decrease the voltage (i.e. being able of consuming power from the DC bus and

hence, having arrows leading from it): the GENSET, the AUX load and PAR load. The AUX and PAR loads, however, are not directly controlled by the driver and are therefore not possible to use for voltage control. Thus, the unit that must be responsible for decreasing the voltage in this case is, once again, the GENSET.

6.2 Control loop migration to PCM

As concluded in the previous section, the TM cannot or must not solely achieve voltage control in cases 2, 3 and 4. In these cases, the GENSET has to assist with or even completely take over the voltage control responsibility from the TM. This implies that some kind of control mode switch has to be performed. Since both voltage control and speed control are realized on subcomponent level in the TCU and GCU respectively, the ability to control for example the internal integral states and thus achieve such a mode switch in a bumpless manner is greatly limited.

One technique to circumvent this restraint and thereby increase the control design freedom is to migrate control loop(s) from the subcomponent controllers to the PCM. This is accomplished by setting the control unit in question to torque control mode and then realizing the actual control loop in the PCM.

6.2.1 Feasibility

Due to the limited communication rate between the PCM and the other control units, it is conceivable that control loop migration may compromise the controllability and may thus not be a feasible solution. The faster the dynamics in the controlled quantity are, the faster the required communication rates are in order to achieve adequate control. The two physical states to be controlled in the powertrain are engine speed ω_{ice} and DC voltage U , of which engine speed is the one having the slower dynamics. Therefore, engine speed control is assessed the more feasible candidate for control loop migration.

6.3 Alternative strategy (CS3)

An alternative approach still working according to the push principle is possible. In this approach, engine speed control is achieved in a novel fashion; engine speed control is mainly carried out by the TM, and the actual control loop is migrated to the PCM as described in Section 6.2. From here on, this strategy is referred to as Control Strategy 3 (CS3).

The main idea with CS3 is the following:

- The GCU operates in voltage control mode.
- The TCU operates in torque control mode and controls the engine speed ω_{ice} through a superior speed controller in PCM.

- The driver demand α_{ap} is interpreted and converted into a torque reference to the ICE. Thus, the ECU operates in torque control mode.

A schematic of this control idea is presented in Figure 6.3. By letting the GEN operate in voltage control mode, the voltage can be controlled independent of the different driving scenarios. The same problems as with CS2 are still present though, but now with engine speed instead of voltage; having the TM control the engine speed still poses an inability to increase and decrease the speed when $v_{veh} = 0$ and $\alpha_{ap} = 0$, respectively. However, migrating the speed controller to the PCM introduces bigger design freedom and therefore greater possibilities to handle these corner cases.

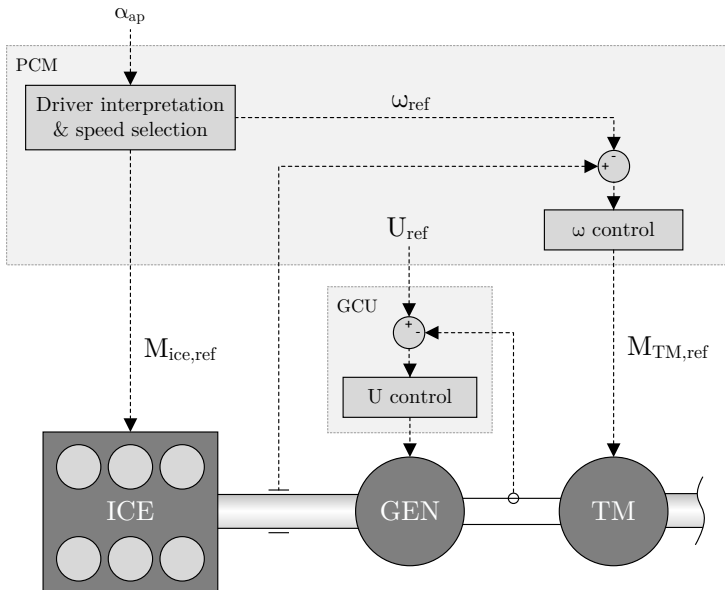


Figure 6.3: Idea of control strategy 3.

6.3.1 Initial idea

CS3 according to this initial idea is implemented in Simulink™ and a vehicle deceleration from 20 km/h to 0 km/h is simulated, with $\alpha_{ap} = 0$ and a constant engine speed reference of 2000 rpm. The results are presented in Figure 6.4.

As seen in the figure, the same standstill problem as with CS2 is still present in CS3 but now with engine speed instead of voltage; when the vehicle speed reaches zero, the engine speed drops as a consequence of the ICE generating a negative torque due to friction and pump losses and the TM is not able to keep it up as it lacks kinetic energy to do so. However, since the ECU has a low idle governor that kicks in when the speed drops below the low idle setpoint, the

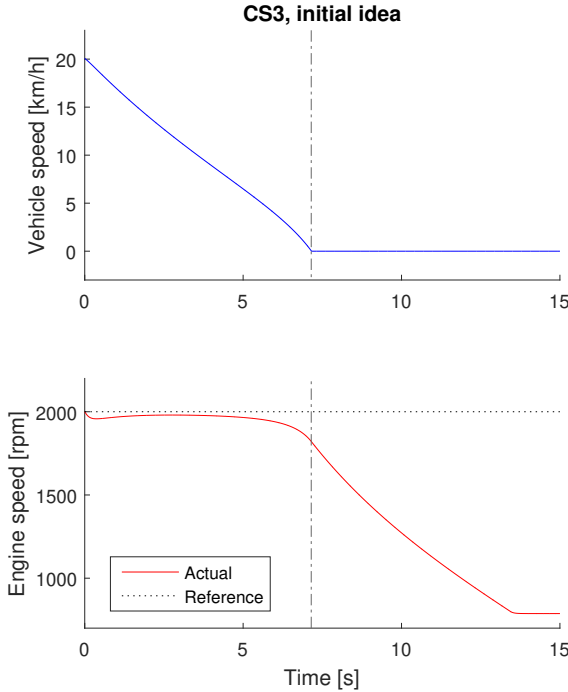


Figure 6.4: Simulation results with the initial idea of CS3 implemented. The vehicle is decelerated from 20 km/h to standstill by setting $\alpha_{ap} = 0$. The engine speed reference is set constant to 2000 rpm.

engine will not stall. Hence, this problem can be solved simply by leaving the speed control to the LIG to take care of during standstill.

The no demand problem, however, still remains. When the driver does not demand any traction, the TM is still not allowed to generate any traction torque and hence, it is unable to decrease the engine speed.

6.3.2 Variable effective controller gains

Another phenomenon visible in Figure 6.4 is how the speed control performance becomes worse as vehicle speed decreases. This can be explained with variable effective controller gains due to the variable gear ratio. When controlling the engine speed with the TM, the control signal from the speed controller is a reference torque to the TM and not directly to the GEN, the component that actually affects the speed. In the DC bus, an electrical gearing occurs causing a torque conversion between control signal and the torque that will effectively load the engine shaft. This electrical gearing can be mathematically derived as

$$P_{GEN} = P_{TM} \quad \Rightarrow \quad M_{GEN}\omega_{GEN} = M_{TM}\omega_{TM}$$

$$\Rightarrow M_{TM} = \frac{\omega_{GEN}}{\omega_{TM}} M_{GEN} \quad (6.1)$$

By defining the effective gear ratio as

$$i_e \equiv \frac{\omega_{GEN}}{\omega_{TM}} \quad (6.2)$$

the following expressions are obtained:

$$M_{TM} = i_e M_{GEN} \Leftrightarrow M_{GEN} = \frac{1}{i_e} M_{TM} \quad (6.3)$$

The equation for the engine speed PI controller yields

$$u(t) = M_{TM} = K_p e(t) + K_i \int e(t) dt \quad (6.4)$$

Combining Equations 6.3 and 6.4 yields

$$M_{GEN} = \frac{1}{i_e} \left(K_p e(t) + K_i \int e(t) dt \right) = \frac{K_p}{i_e} e(t) + \frac{K_i}{i_e} \int e(t) dt \quad (6.5)$$

From this equation, it is clear that the controller gains will vary with the effective gear ratio.

6.4 Gear ratio compensated control signal

The effect of variable controller gains can be counteracted by introducing control signal compensation using the effective gear ratio, that is

$$u_{comp} = i_e u_{uncomp} \quad (6.6)$$

where u_{comp} and u_{uncomp} are the compensated and uncompensated control signals, respectively.

6.4.1 Deceleration from 20 km/h to standstill

Simulation results for a deceleration from 20 km/h to standstill after introducing this compensation are shown in Figure 6.5. When comparing these results to the same deceleration without control signal compensation in Figure 6.4, it is evident that by introducing the compensation, speed control performance is constant until the vehicle stops.

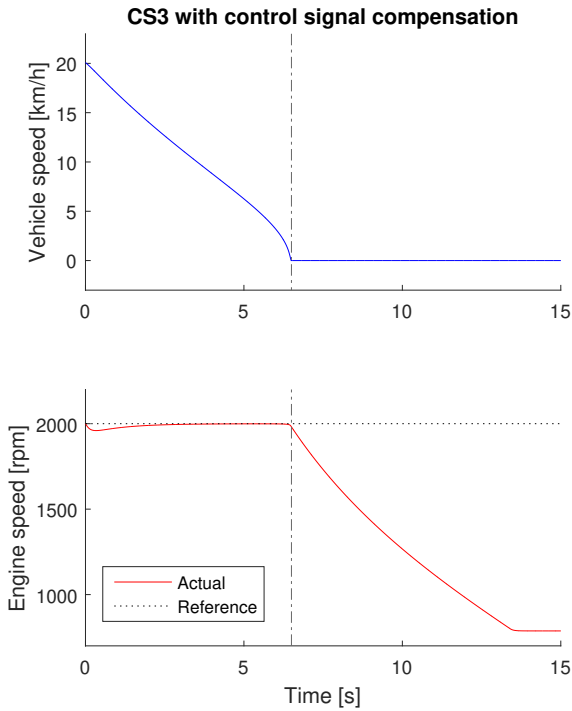


Figure 6.5: The same simulation as in Figure 6.4 is run, but with the control signal compensated for the varying effective gear ratio.

6.4.2 Full drive cycle

In Figure 6.6, the full drive cycle is simulated with control signal compensation implemented and a constant speed reference of 2300 rpm. The driver demand is interpreted into a demanded power simply as $P_{dem} = \alpha_{ap} P_{max,nom}$.

One major problem is obvious: the TM never delivers the full demanded power. This can be explained with the driver interpretation not compensating friction and pump losses in the engine, causing the actual delivered power to be lower than the demanded power.

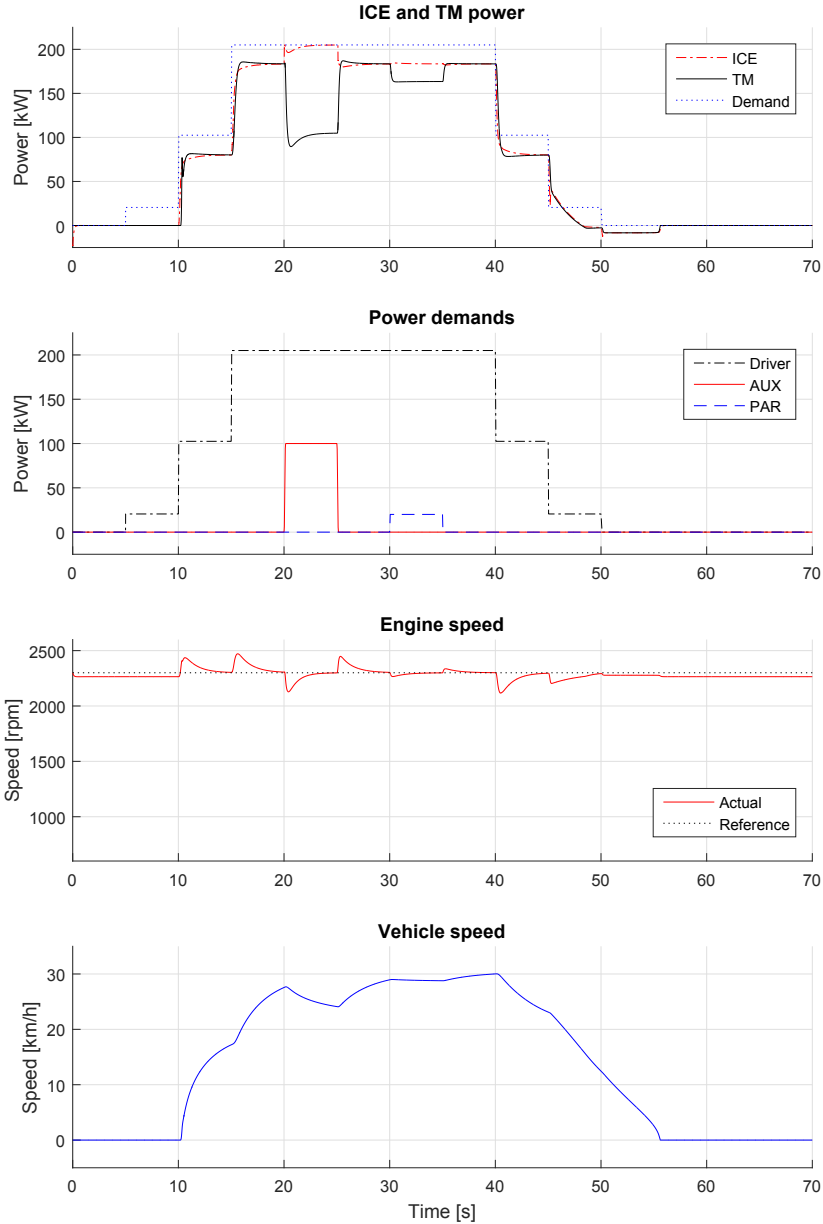


Figure 6.6: Simulation results for the full fictive drive cycle with CS3 with control signal compensation implemented.

6.5 Friction and pump loss compensation

Since the requested torque from the engine is an indicated torque, the actual braking torque on the shaft is lower due to friction and pump losses. In order to make the engine produce full power at maximum accelerator pedal position, these losses have to be compensated for. One way of doing this is by approximating the losses and offset the ICE torque reference with this value, that is

$$M_{ice,ref} = \frac{P_{dem}}{\omega_{ice}} + \hat{M}_{loss}(\omega_{ice}) \quad (6.7)$$

In this way, the engine would produce around 0 kW braking power at $\alpha_{ap} = 0$ and around P_{max} at $\alpha_{ap} = 1$.

6.5.1 Engine braking

In order to spare the mechanical brakes and hence reduce maintenance costs, engine braking is a desired feature. One drawback with friction compensation in the manner described above is that engine braking will be disabled by design. This can be explained with the following example.

Imagine a case when $v_{veh} > 0$ and $\alpha_{ap} = 0$. The desired behavior is that the TM regenerates power into the DC bus and consequently brakes the vehicle. Power regeneration from the TM, which is the speed controlling unit, occurs when the engine speed is lower than the reference. If engine losses are not compensated, $\alpha_{ap} = 0$ will imply a negative braking torque from the ICE. This torque will decelerate the shaft, which the TM will try to compensate through feeding power back through the powertrain and effectively engine braking the vehicle.

If, on the other hand, engine losses are compensated for, $\alpha_{ap} = 0$ will imply around zero net engine torque and consequently not cause shaft deceleration. Engine braking will thus not occur.

One possible approach to compensate the losses while still preserving the engine braking capability is to use a multiplication compensation factor in the driver interpretation instead of adding a compensation offset to the ICE reference torque. By approximating the losses at maximum engine speed and adding this to maximum engine power, a compensation factor can be formed as

$$P_{comp} = \alpha_{ap}(P_{max} + P_{fric}(\omega_{max})) = \alpha_{ap}P_{max} \left(\frac{P_{fric}(\omega_{max})}{P_{max}} + 1 \right) \quad (6.8)$$

This way, $\alpha_{ap} = 1$ will cause maximum engine power to be produced, while $\alpha_{ap} = 0$ will still imply a negative braking torque and thus engine braking.

Figure 6.7 shows the simulation results from the full drive cycle with friction compensated driver interpretation. As seen in this figure, the powertrain does deliver the full demanded power at $\alpha_{ap} = 1$, but produces lower-than-requested powers for lower α_{ap} . This can be explained with the way the friction compensation is achieved. In Equation 6.8, the term $\frac{P_{fric}(\omega_{max})}{P_{max}}$ estimates the ratio between friction power and maximum power at *maximum speed* in order to reach full

power at full driver demand. At lower loads this ratio is typically bigger and hence, the compensation is not sufficient (clearly visible at 5-10 s when $\alpha_{ap} = 0.1$ but still no traction power is delivered). This is a drawback with the selected loss compensation technique. However, this problem is less significant with a more sophisticated engine speed reference selection technique implemented (keeping the engine speed reference at a constant high level as in this simulation is not very rational), which will be evident in later sections.

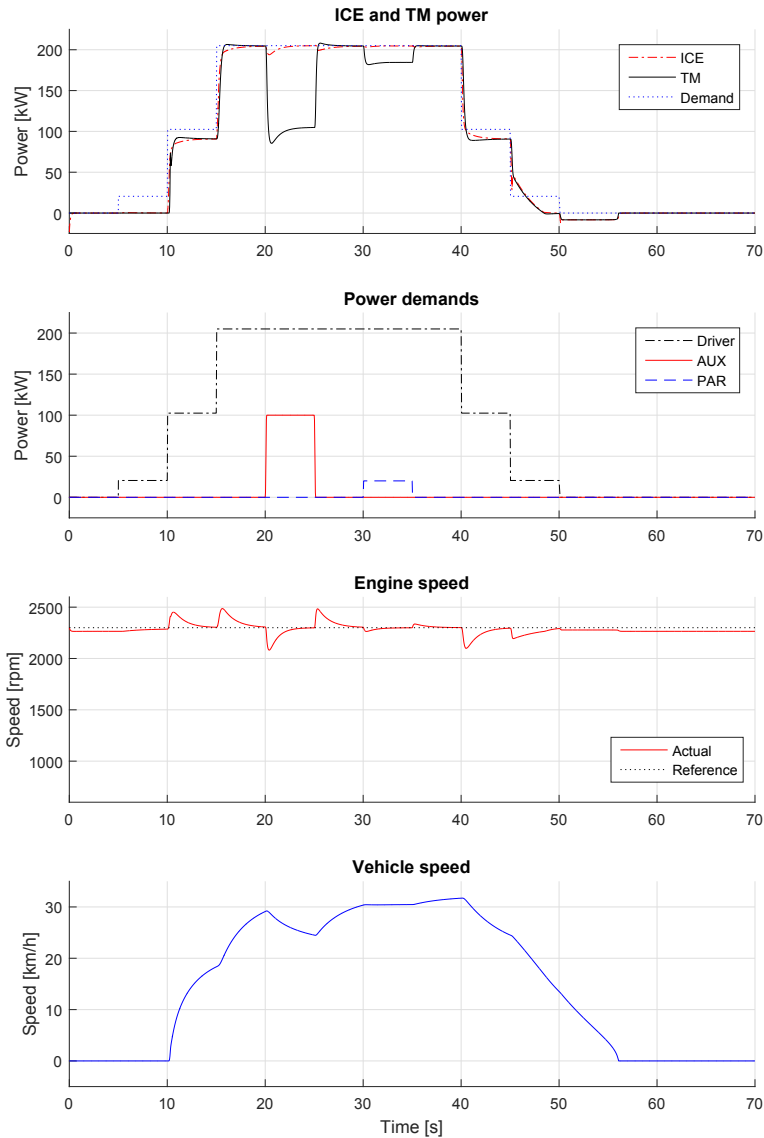


Figure 6.7: Driver interpretation using friction compensation factor.

6.6 Speed reference selection

Selecting an appropriate engine speed reference is not trivial. In the previous simulations, the speed reference has been set to a constant, high value in order to isolate the studied problems. However, running the engine constantly at high speed is of course not an option for several reasons, for example low efficiency at part load and increased engine wear.

One way to achieve dynamic speed reference selection is to use a lookup map from requested power to appropriate engine speed. A natural starting point when forming such a map is to select the fuel optimal setpoints in order to minimize fuel consumption. These points are shown as the red, dash-dotted line in Figure 6.8. However, since this line coincides with the maximum ICE power line (black, dotted line in the same figure) for powers above 160 kW, there is no margin to perform an instantaneous increase of produced power without speeding up the engine first. For this reason, the chosen setpoints are offset from the optimal ones as a compromise between fuel economy and power response. Such a compromise, originating from previous work with the powertrain at BAE Systems Hägglunds, is seen as the blue, solid line in Figure 6.8.

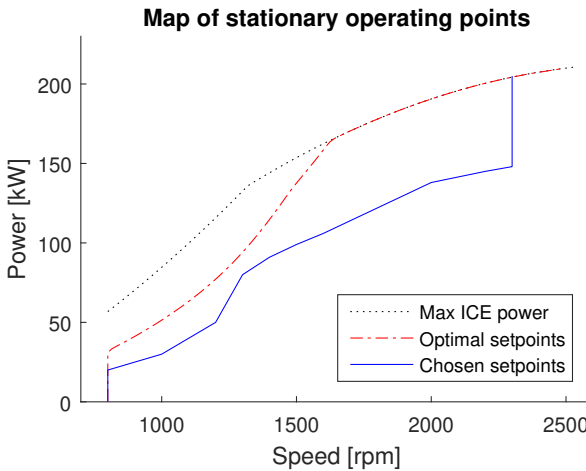


Figure 6.8: Map of operating points.

6.6.1 Reference directly from map

The most basic approach to achieve variable speed reference using the operating point map is simply to choose the reference straight from the map. That is, the demanded engine power is directly translated into an appropriate engine speed, in the following way:

$$\omega_{ref} = f_{map}(P_{dem} + P_{aux}) \quad (6.9)$$

This approach does, however, cause very jerky traction. In Figure 6.9, simulation results with this technique implemented are presented.

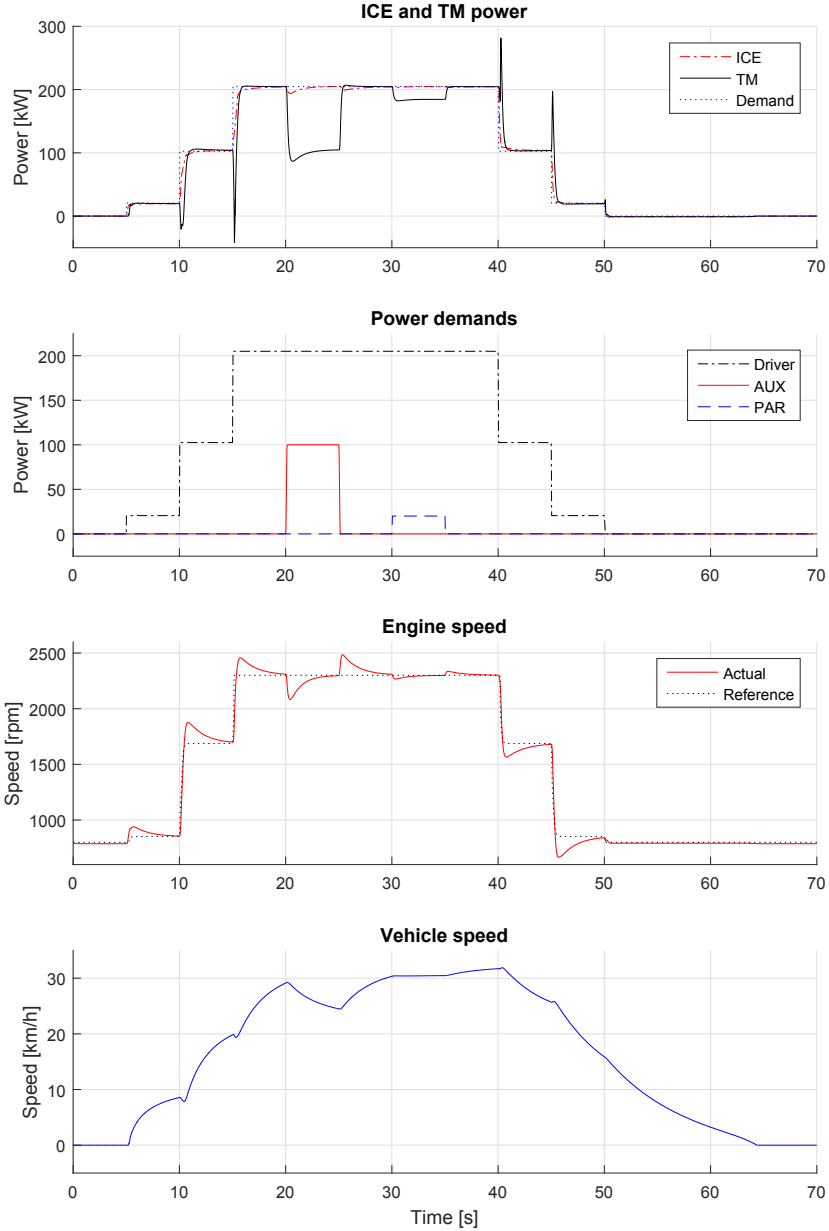


Figure 6.9: Full drive cycle with speed reference directly from operating point map.

As seen in this figure, when α_{ap} is increased (at 10 s and 15 s) TM power decreases initially and then increases to the desired level. This can also be seen in the vehicle speed plot where it is obvious that the vehicle decelerates before starting to accelerate. When α_{ap} is decreased (at 40 s, 45 s and 50 s) the opposite phenomenon occurs; when the accelerator pedal is let up, the traction quickly increases before decreasing. These jerks will be perceived as unintuitive to a driver (*pushing down* the accelerator pedal and the vehicle starts to *decelerate*) and can also be hazardous from a safety perspective and are thus unwanted.

However, Figure 6.9 also reveals a positive characteristic with the dynamic speed reference selection technique; the delivered traction power now matches the desired power. This was not the case in Figure 6.7, which was explained with the compensation factor $\frac{P_{fric}(\omega_{max})}{P_{max}}$ in Equation 6.8 not being sufficient for low loads while having a constantly high engine speed. At lower speeds the engine friction is also lower, making this compensation factor better match the true ratio between friction power at the current speed and maximum engine power. Sufficient compensation is therefore achieved.

6.6.2 Limited shaft acceleration torque

The jerks can be explained with the rapidly increasing speed reference. With increasing speed error, the torque needed to accelerate the shaft increases and thus, less torque is available for traction. One way to circumvent this phenomenon is to limit the torque used for shaft acceleration.

The torque produced by the ICE can be used for two purposes: shaft acceleration or further transmission through the powertrain, ultimately being used for traction or external loads. This is visualized in Figure 6.10.

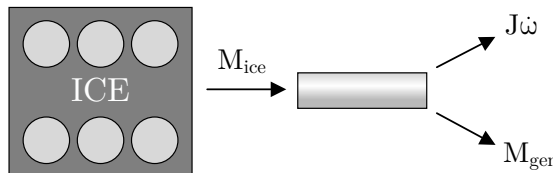


Figure 6.10: Illustration of consumers of the ICE torque.

When choosing speed reference directly from the operating point map as in Section 6.6.1, the rate of change in engine speed is basically infinite during transients. That is, more or less all engine torque is used to accelerate the shaft, causing the jerky transients. In order to control the amount of torque used for shaft acceleration, the rate of change (i.e. the desired acceleration) can be limited. The torque needed for this acceleration can be expressed using Newton's second law for rotation as

$$M_{acc} = J_{genset}\dot{\omega}_{ice} \quad (6.10)$$

where M_{acc} is the shaft acceleration torque, J_{genset} the moment of inertia of the

genset and $\dot{\omega}_{ice}$ the shaft acceleration. By limiting the accelerating torque to a certain portion of the torque produced by the engine according to

$$M_{acc} = \beta M_{ice}, \quad 0 < \beta < 1 \quad (6.11)$$

the balance between the two consumers can be controlled. Combining the two equations above yields an expression for the corresponding speed reference rate of change limit as

$$\dot{\omega}_{ice} = \frac{\beta M_{ice}}{J_{genset}} \quad (6.12)$$

This limit is implemented in Simulink™ using a dynamic rate limiter, as shown in Figure 6.11. In addition to the rate limiter, a filter is added in order to smoothen the reference signal and thereby further prevent bumpy traction.

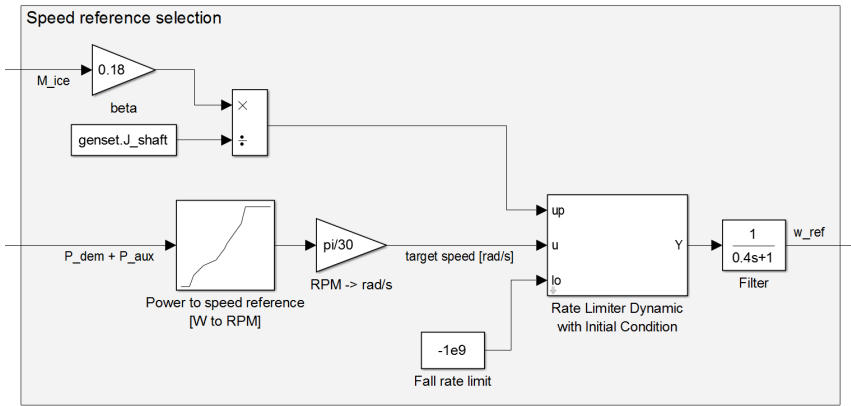


Figure 6.11: Simulink™ implementation of rate limited speed reference selection.

Simulation results with this technique implemented are shown in Figure 6.12. As seen, the jerks are significantly reduced or even removed. Comparing the speed reference curve in this case with speed reference selection directly from the map (Figure 6.9), it is also obvious that the reference transients are slower.

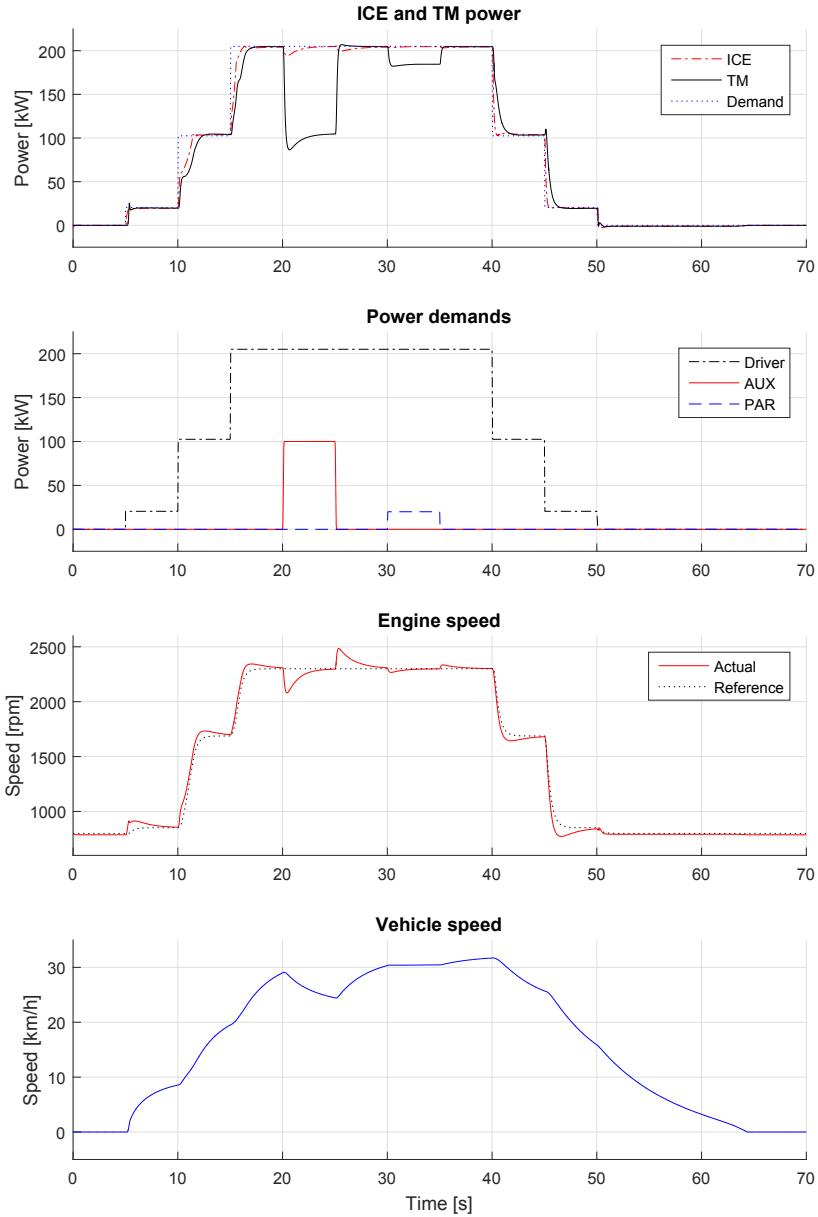


Figure 6.12: Simulation results after implementing the rate limited speed reference selection.

6.7 Traction power limit with ICE torque reduction

From studying how the traction power follows the reference, it is obvious that the power drops off rather slowly after releasing the accelerator pedal. This is shown in more detail in Figure 6.13. As seen, it takes over one second for the traction power to reach its stationary value after the accelerator pedal is let up. This is not desired for safety reasons; when the accelerator pedal is released, traction should be instantly decreased of course.

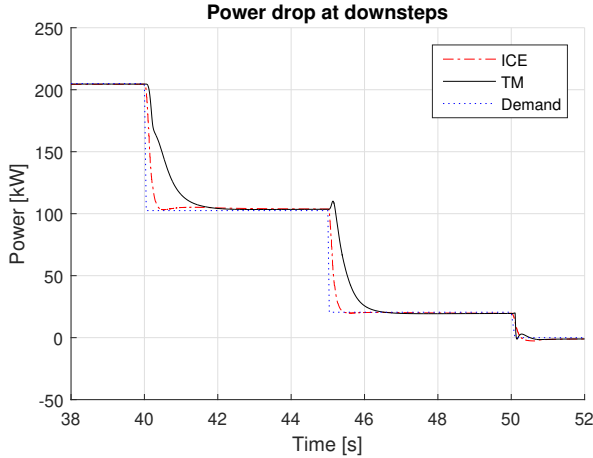


Figure 6.13: Enlarged view of Figure 6.12, emphasising the slow power drop.

One way to handle both the slow drop off problem shown in Figure 6.13 and also the no demand problem is to introduce the demanded power as an upper saturation limit on the TM power, that is

$$P_{tm} = \min(M_u \omega_d, P_{dem}) \quad (6.13)$$

where P_{tm} is the TM power, M_u the torque demanded by the speed controller and P_{dem} the power demanded by the driver. Introducing this limit compromises speed control though. Since the TM in the speed controlling actuator, limiting its motoring power also limits its ability to decrease the engine speed. The two units able to affect the speed is the GEN/TM and the ICE, so if the GEN/TM cannot decrease the speed, then the ICE must do it. Recall Newton's second law for rotation as stated in Equation 5.7. If both M_{gen} and J are not controllable, then the only way to alter ω is through M_{ice} . Thus, one way to handle this problem is to reduce the ICE torque when the TM power saturates. This approach is described in [14], even though it is slightly different since it uses the GEN and not the TM as the speed controlling unit.

The approach can be described with

$$M_{ice,ref} = \frac{P_{dem}}{\omega_{ice}} - k_{p,red} M_{clip} \quad (6.14)$$

$$M_{clip} = \begin{cases} M_u - M_{sat}, & \text{if } M_u - M_{sat} > 0 \\ 0, & \text{otherwise} \end{cases} \quad (6.15)$$

$$M_{sat} = \frac{P_{dem}}{\omega_d} \quad (6.16)$$

Simulation results with this technique implemented are presented in Figures 6.14 (detailed view) and 6.15 (full drive cycle). With this approach, the delivered power strictly follows the demanded power at the downsteps. It is also obvious how the ICE compensates by reducing the power when the TM power is clipped.

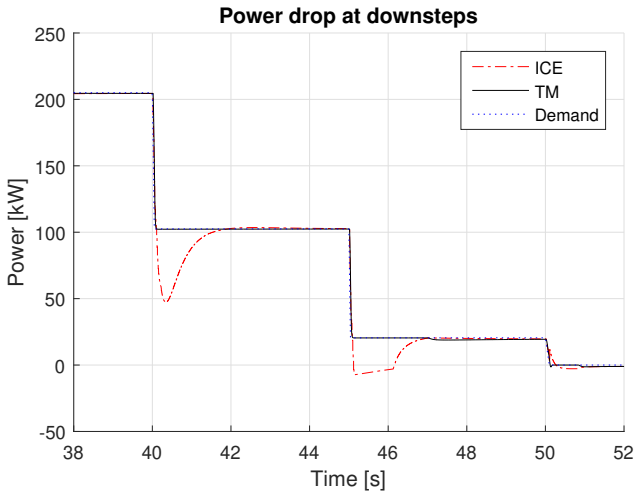


Figure 6.14: Power drop with TM power limit and ICE torque reduction implemented.

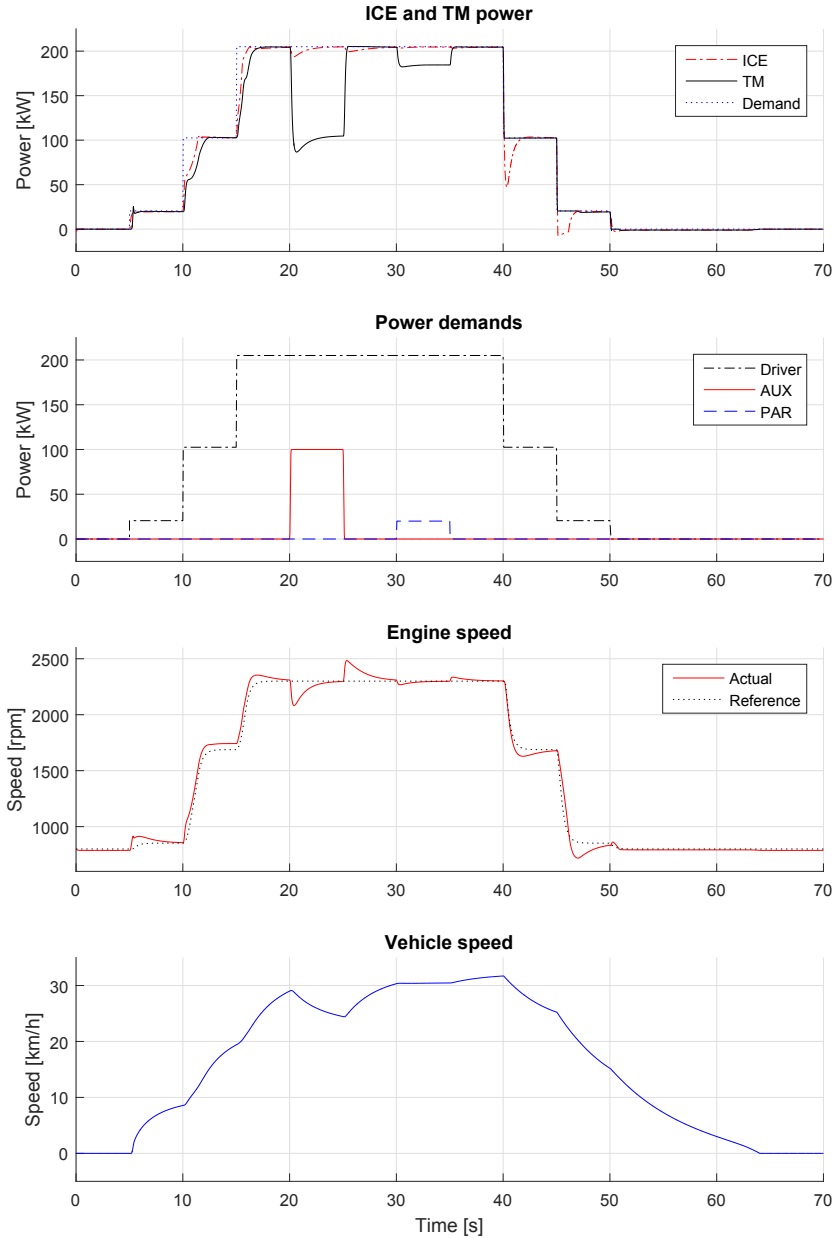


Figure 6.15: Simulation results when having the maximum TM limit and ICE torque reduction implemented.

6.8 Conditional idle speed setting

As visible in Figure 6.15, the vehicle does not engine brake when the accelerator pedal is released. This is obvious from the ICE power being zero at $\alpha_{ap} = 0$, when the desired behavior is $P_{ice} < 0$.

This can be explained using the LIG. In the simulation run in Figure 6.15, the low idle speed setpoint is 800 rpm. Thus, when the speed reference selection algorithm chooses the same 800 rpm as reference for the speed controller and the speed falls below this point, the LIG will counteract this speed error instead of the regular speed controller doing it. Consequently, no engine braking will occur.

In order to circumvent this problem, the LIG speed setpoint can be offset using a deadband when the vehicle is moving, according to

$$\omega_{ref,LIG} = \begin{cases} \omega_{ref,LIG,des} - \omega_{db,LIG}, & \text{if } v_{veh} > 0 \\ \omega_{ref,LIG,des}, & \text{otherwise} \end{cases} \quad (6.17)$$

where $\omega_{ref,LIG}$ is the effective speed reference to the LIG, $\omega_{ref,LIG,des}$ the desired setpoint and $\omega_{db,LIG}$ the deadband.

Simulation results with this technique implemented and a deadband of 200 rpm are presented in Figures 6.16 (detailed view) and 6.17 (full drive cycle). As seen in these results, the engine consumes power when $v_{veh} > 0$ and $\alpha_{ap} = 0$ (i.e. between 50 s and 60 s), which is visible both in the power graphs and from comparing the vehicle deceleration in this case with the case in Figure 6.15. Without the conditional idle speed setting, a deceleration from 15 km/h to standstill takes approximately 14 s, compared to 11 s in this case.

However the braking power the engine consumes is very low, just around 2.5 kW. This is due to the low engine speed during braking which implies low engine friction. If a higher speed reference was retained throughout the braking procedure, the increased friction would lead to more powerful engine braking.

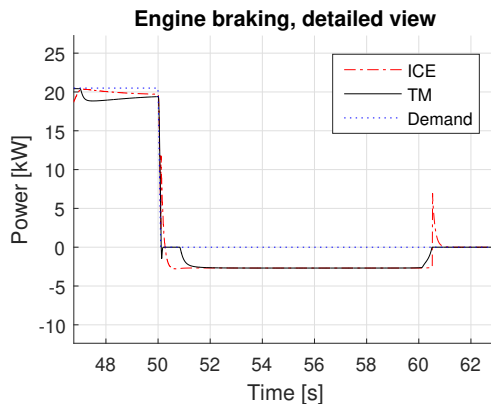


Figure 6.16: Detailed view of Figure 6.17, emphasizing that the conditional idle speed setpoint technique enables engine braking.

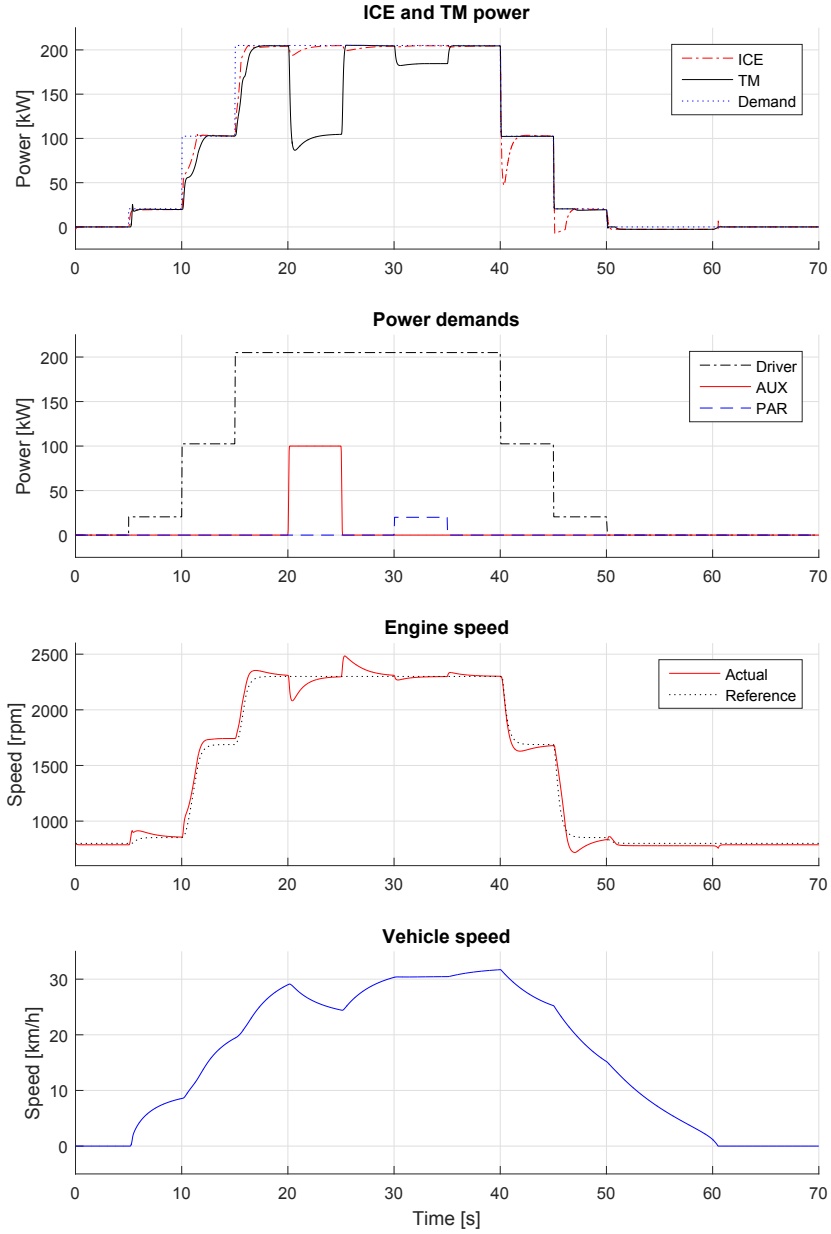


Figure 6.17: Simulation results with the conditional idle speed setpoint technique implemented.

6.9 Infinite torque gain

Refer to Equation 6.2 describing the effective gear ratio. With decreasing vehicle speed (and thus TM speed), the effective gear ratio increases. When the speed approaches zero, the gear ratio grows to infinity, that is

$$\lim_{\omega_{TM} \rightarrow 0^+} i_e = \lim_{\omega_{TM} \rightarrow 0^+} \frac{\omega_{GEN}}{\omega_{TM}} = \infty \quad (6.18)$$

An infinite effective gear ratio implies infinite gain from ICE torque to TM torque. In other words, when the vehicle stands still and the driver just slightly touches the accelerator pedal, the TM will initially deliver maximum torque. This is confirmed in simulation, which is shown in Figure 6.18 where the torque curve from the simulation presented in Figure 6.17 is shown. As visible, the torque quickly peaks at 5 s, even though the driver only requests 10% traction power.

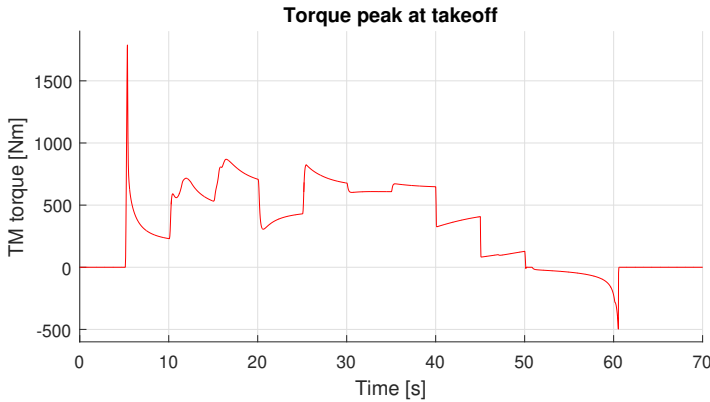


Figure 6.18: TM torque peak at takeoff, due to infinite effective gear ratio.

6.9.1 Takeoff strategy

To handle the effect of infinite effective gear ratio, a takeoff strategy is necessary. Otherwise, driving at low speeds will be highly difficult. Several possible takeoff techniques are identified.

- **Uncompensated control signal**

The purpose of the control signal compensation described in Section 6.4 is to ensure constant speed control performance independent of vehicle speed. This comes with the disadvantage of high torques at low vehicle speeds, though. By accepting variable speed control performance, a smoother takeoff can be achieved by using a non-compensated control signal.

- **Mode switch**

Utilizing a pull control strategy at takeoff lets the driver directly control

the actual traction torque which allows for more precise low speed driving. Then switching mode to a push strategy at higher speeds enables the advantages of this approach.

- **TM torque limit at low speeds**

An approach similar to the one described in Section 6.7 could be used; by limiting the traction torque at low speeds and compensating the ICE torque accordingly, a softer takeoff could be realized.

Uncompensated control signal

The uncompensated control signal technique is implemented, and the simulation results presented in Figure 6.19 for both compensated and uncompensated control signal. As shown, the torque response when not using control signal compensation is much smoother than the compensated response. However, the smoother takeoff torque comes at a cost of reduced speed control performance, which is obvious from comparing the engine speed plots for the two cases.

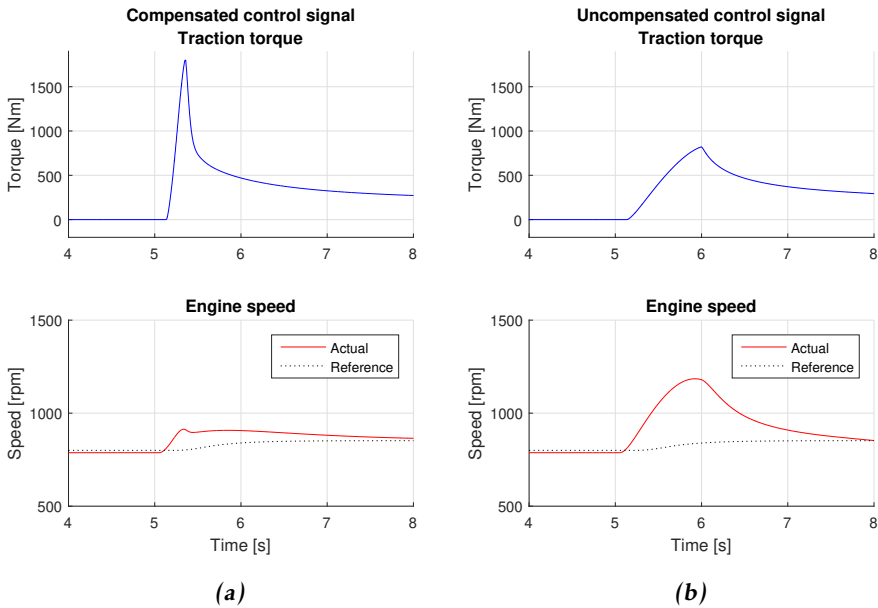


Figure 6.19: Traction torque and engine speed during takeoff for (a) compensated and (b) uncompensated control signals.

7

Results

In this chapter, the final control strategy is presented together with the simulation results with this strategy implemented.

7.1 Final control strategy

The final control strategy works according to CS3 and makes use of the following techniques, as described in the previous chapter.

- Driver interpretation using engine loss compensation as described in Section 6.5
- Speed reference selection with limited shaft acceleration torque as described in Section 6.6.2
- Traction power limit with ICE torque reduction according to Section 6.7
- Conditional idle speed setting as described in Section 6.8
- Uncompensated speed control signal as takeoff strategy as explained in Section 6.9.1

A block diagram of this strategy is presented in Figure 7.1.

7.1.1 Parameters

With this strategy, there are four strategy-specific tuning parameters.

- Proportion of demanded torque that should be allowed for shaft acceleration, β

- Time constant for the speed reference low-pass filter
- Proportional reduction factor for clipped TM torque, $k_{p,red}$
- Deadband for the conditional idle speed setpoint, ω_{db}

Additionally, the parameters for the speed controller in the PCM and the voltage controller in the GCU have to be tuned.

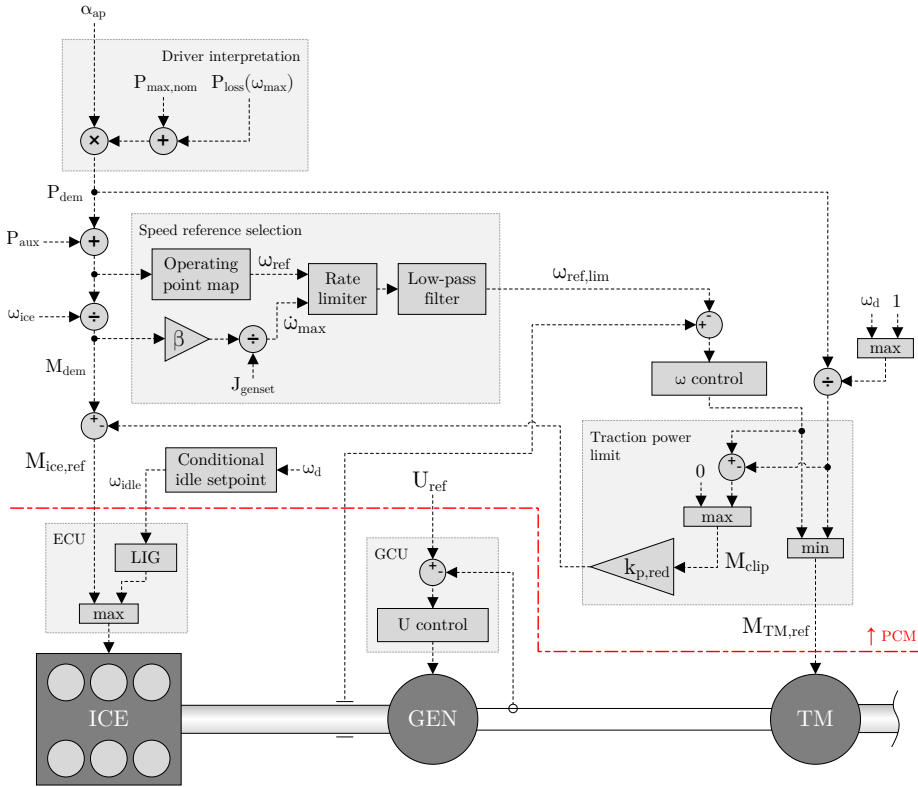


Figure 7.1: Block diagram of the final control strategy. Logic above the red, dash-dotted line is implemented in the PCM and logic below is realized in the subcomponent control units. Note that necessary integrator anti-windup features in the speed controller are omitted in this diagram. Furthermore, the $\max(\omega_d, 1)$ selector on the very right in the figure is added in order to prevent division by zero at standstill.

7.2 Simulation results

Simulation results from the three following cases are presented.

- Fictive drive cycle with full ICE performance
- Fictive drive cycle with ICE performance reduced by 30%
- Real drive cycle with full ICE performance

These results are presented objectively in this section, and are then discussed in the next chapter.

7.2.1 Fictive drive cycle, 100% ICE performance

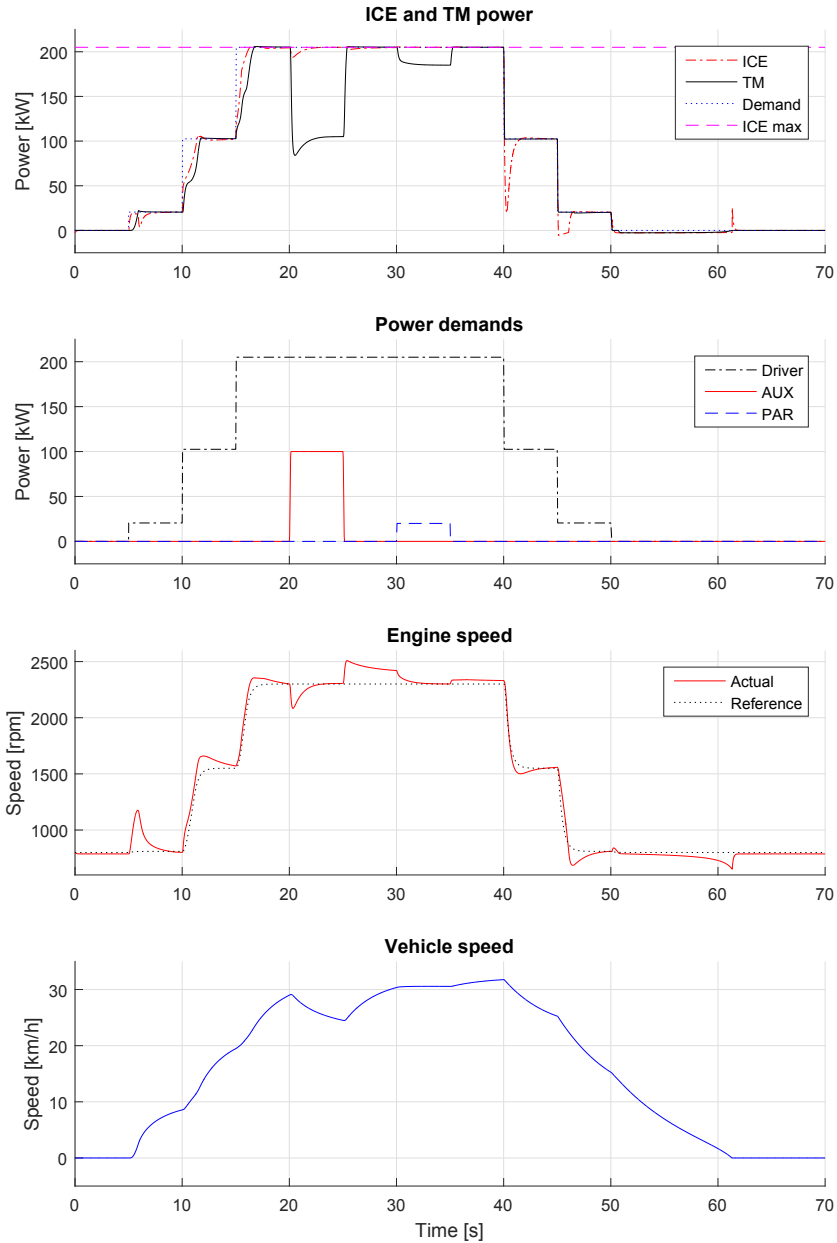


Figure 7.2: The final control strategy running the fictive drive cycle with full ICE performance.

7.2.2 Fictive drive cycle, 70% ICE performance

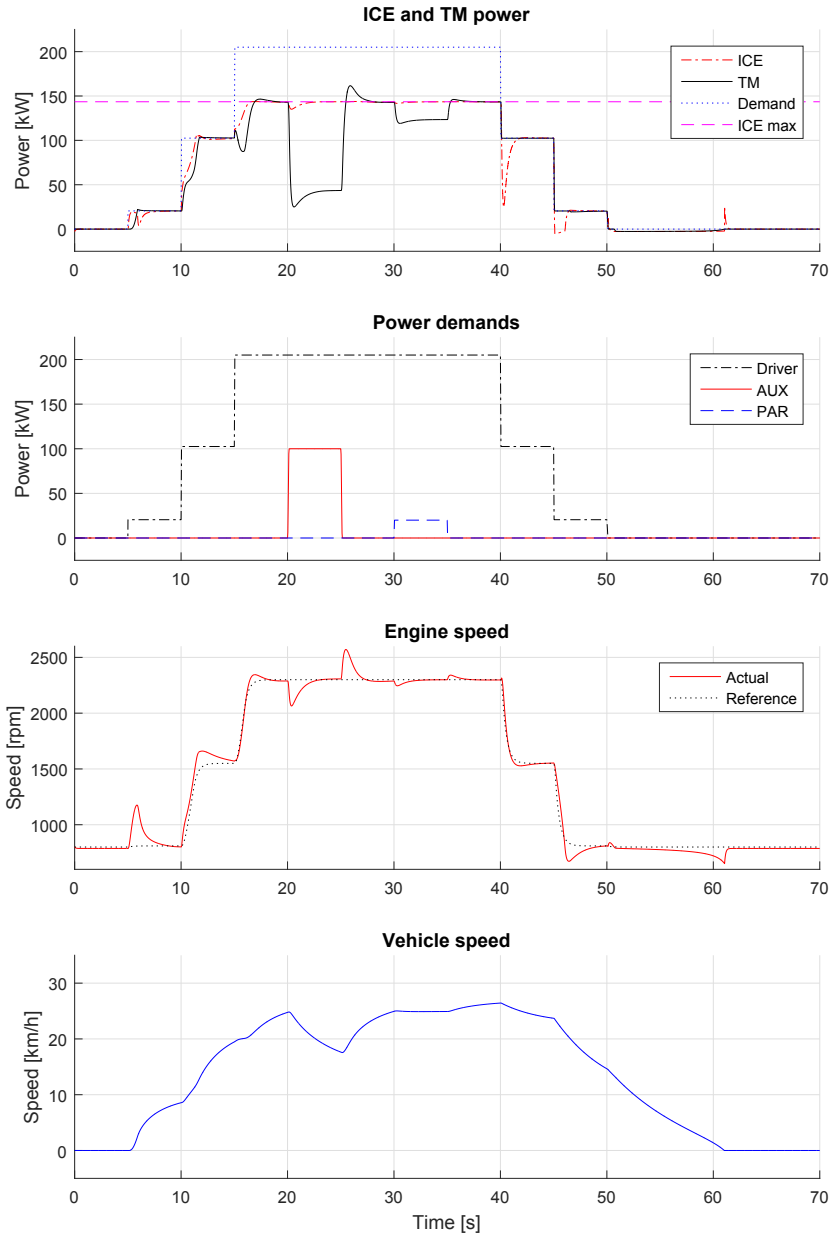


Figure 7.3: The final control strategy running the fictive drive cycle with 30% reduced engine performance.

7.2.3 Real drive cycle

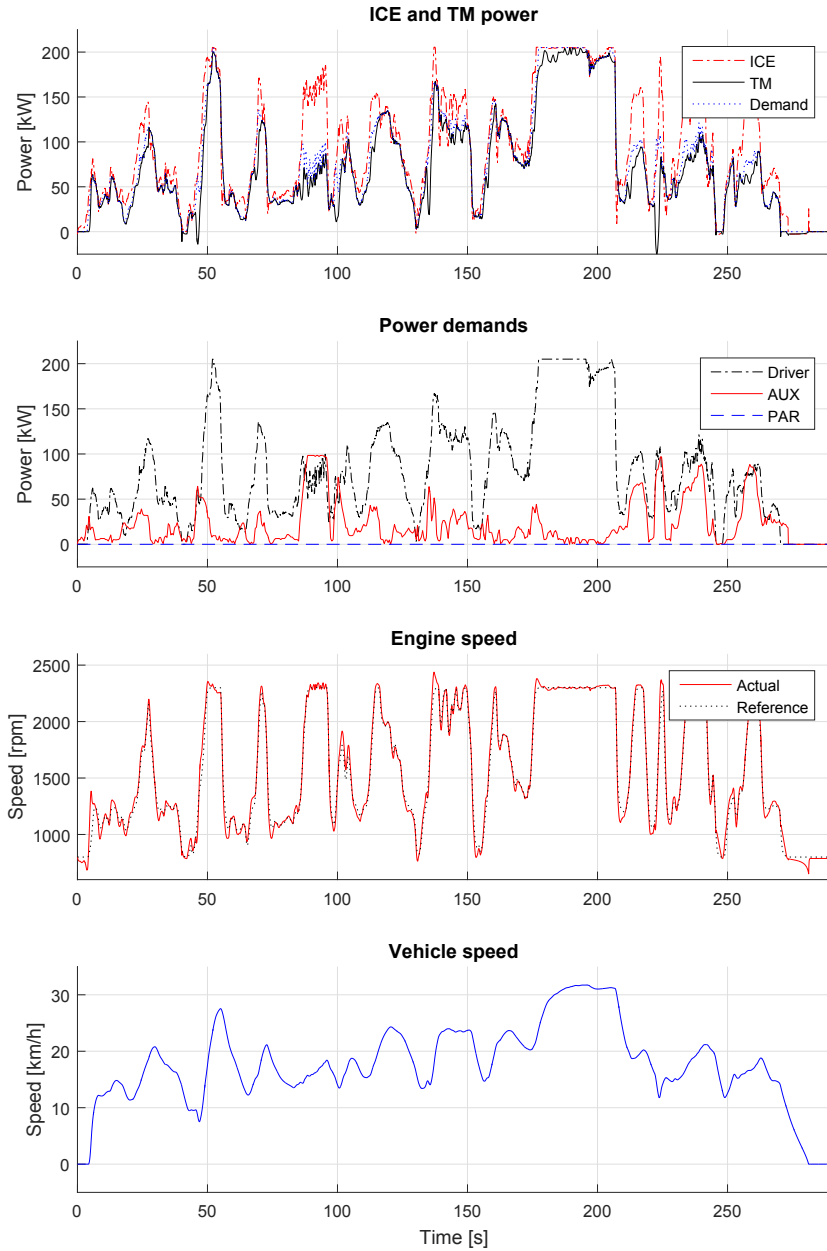


Figure 7.4: The final control strategy running the real drive cycle.

8

Discussion

8.1 Results

In this section, the results from the previous chapter are discussed. First of all, from studying Figure 7.3 it is clear that the developed strategy solves the original maximum engine power utilization problem; when the driver demands more power than available from the engine, maximum available power is delivered in line with the desired behavior. However, when comparing these results to the ones presented in Figure 7.2 when the full engine power is available, it is noticed that the introduced power reduction causes bumpy traction (occurring during the transient at 15-16 s). This speaks for the basic speed reference selection strategy used not being robust enough to handle changing engine performance. Hence, a more sophisticated algorithm is needed in order to prevent these bumps.

8.1.1 Jerks during real drive cycle

In Figure 7.4, the results from the final strategy running the real drive cycle are shown. As seen, there are still some traction jerks occurring, even though a speed reference selection strategy aimed to prevent this is used. In Figure 8.1, detailed plots from the final strategy running the real drive cycle are shown. In these plots, three obvious occurrences of jerky traction are present at 46 s, 212 s and 222 s. All these jerks have in common that they occur when the AUX load (dashed, black line) quickly increases. This is reasonable since the AUX loads occur instantly and start to consume power from the DC bus, faster than the ICE can compensate the load by increasing the produced power. Hence, less power will be available for traction initially and a jerk will occur.

This behavior might be acceptable to the driver, though. When starting to consume power with an external load, for example using the hydraulics, it is rather

intuitive that traction power shortly decreases to give room for the introduced load. Thus, the severity of this issue is maybe not the highest.

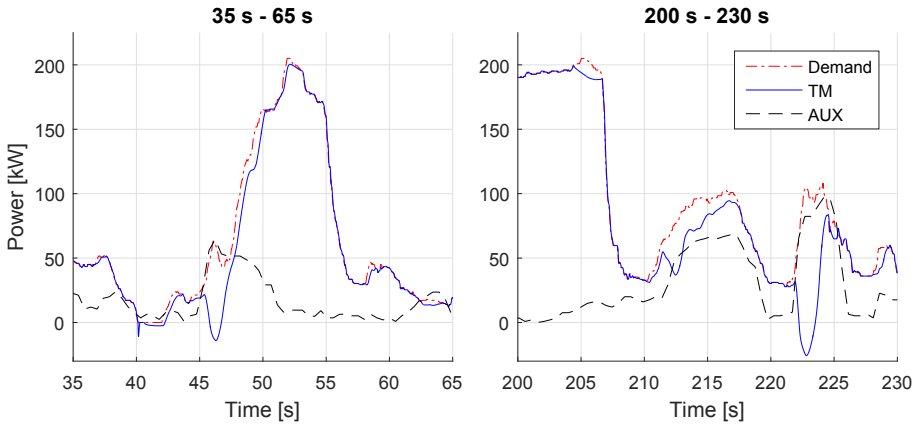


Figure 8.1: Detailed plots from the simulation presented in Figure 7.4 emphasizing three occurrences with jerky traction (46 s, 212 s and 222 s).

8.1.2 Natural priority handling

In the results, it is seen that the push strategy handles load priority in a natural way. As stated in Chapter 1, the requirement is that external loads should take precedence over traction when they occur. From studying Figures 7.2 and 7.3 at 20 s and 30 s when AUX and PAR loads appear while maximum traction power is being delivered, it is seen that traction power is naturally decreased, giving room for the external loads. This happens without having any priority-specific logic implemented, which is seen as an advantage with this approach.

8.1.3 Uncertain applicability of real drive cycle signals

The recorded signals used as the real drive cycle are recorded on a vehicle which uses a control strategy based on a torque request from the driver. In the developed strategy on the other hand, the driver demand is interpreted as a desired power. This difference may jeopardize the applicability of the recorded driver signals on the studied case since it is highly probable that the driver would behave differently in the two cases. For example, assume the driver desires a constant acceleration of the vehicle (i.e. a constant traction torque). In the case with a torque based request, the driver would simply keep the accelerator pedal at a constant position. However in the case with a power based request, a constant accelerator pedal position would imply constant power and hence a continuously decreasing traction torque due to the increasing vehicle speed. This is obvious in the torque curve shown in Figure 6.18. For this reason, the driver would gradually increase the accelerator pedal position in order to counteract this phenomenon, effectively

working as a constant torque controller. It is thus conceivable that the accelerator pedal position signal in a case when a power based driver interpretation is used could differ significantly from the torque based scenario, consequently making the applicability of the recorded drive cycle questionable.

8.2 Modeling

In this section, topics regarding the developed powertrain model are discussed.

8.2.1 Limited model validation

Since no recorded data from the studied powertrain has been available, no model validation against real measurements has been possible. This is of course a significant shortcoming in the work, limiting the credibility in the conclusions drawn. However, since the studied topic of the thesis is conceptual control strategies and general characteristics rather than how the actual powertrain performs, the conclusions are still regarded trustworthy.

As data from the real powertrain becomes available in the future, validating and improving the model as necessary is suggested as prospective work.

8.2.2 Simplified component models

Many assumptions and simplifications have been made throughout the modeling work. Two components that have been greatly simplified are the electric machines (generator and traction motor), which are modeled as first-order systems. This simplification is motivated with the fact that the dynamics of the electric machines are considerably faster than the dynamics of the ICE, which makes the ICE the limiting component. If this simplification would be well off reality, it is conceivable that the real powertrain would behave significantly differently than the modeled one and that other, undiscovered phenomena would occur.

Furthermore, an aspect that has not been taken into consideration is the losses in the power electronics. Since these losses are not modeled, the inverters are effectively assumed to be loss-free. Having a small portion of the power dissipating in these components would of course affect the powertrain performance, but it is questionable whether it would alter the principal behavior of the powertrain or not. Also, since a parasitic load connected to the DC bus is modeled, this disturbance can be seen as rather equivalent to the inverter losses except for the magnitude of the power.

8.3 General discussion

This section discusses general aspects of the control strategy development work.

8.3.1 Speed control dynamics affecting traction

When the established pull strategy is used, the driver is in direct control of the traction torque, while engine speed control is achieved by a controller. In this way, the dynamics from the speed control (for example sudden torque transients) affect the ICE and not the TM. This will be noticed by the driver only aurally as variances in engine speed, while traction typically remains unaffected.

When using the push approach, however, the driver is no longer in direct control of the traction, but controls it indirectly through the engine power, while the TM controls the engine speed (in the case of CS3). This causes traction, which is the ultimate objective of the whole system, to be *an effect* of a control loop instead of being directly driver initiated. The dynamics from the speed control will therefore affect the traction instead of the engine, which is disadvantageous from a drivability perspective.

The problem with traction jerks discussed above is a result from this characteristic. In order to achieve smooth traction using the push principle, a good engine speed reference selection technique is needed.

8.3.2 Driver interpretation using traction torque

Throughout the thesis, the driver demand is interpreted as a requested engine power. As a consequence, the traction torque will decrease with increasing vehicle speed for a constant accelerator pedal position. This is visible for example in Figure 6.18, where the sawtooth-like shape of the torque curve is an effect of this characteristic.

This approach is not the obvious solution though. An alternative technique is to interpret the driver demand as a requested traction torque, and then calculate which ICE torque this corresponds to. However, there is one major problem involved with this approach: at standstill, the effective gear ratio and thus the torque gain from ICE torque to TM torque is infinite as shown in Equation 6.18, making it difficult to achieve the desired traction torque for low speeds. Still, this problem is already present with the power interpretation as implemented in this thesis, speaking for a driver interpretation based on traction torque not being more difficult than the power-based counterpart.

8.3.3 CS1 with control loop migration

In CS3, the engine speed control loop is migrated to the PCM. This migration enables greater control design freedom. In the established CS1, engine speed control is achieved by the ECU. If this control loop was migrated to the PCM as well, the traditional CS1 could possibly be improved. Such a migration would for example enable the possibility to add a feed-forward part to the control loop,

something that is not possible with today's established strategy. Adding a feed-forward part could make the ICE respond faster when a traction demand occurs and hence improve the response of the whole powertrain.

8.3.4 Benefits of energy storage

As stated in the Delimitations section, adding an energy storage to the powertrain has not been an option during this thesis. However, it has to be mentioned that adding such a feature would enable at least two advantages.

- **Reduced fuel consumption** - Adding an energy storage would enable the possibility to take care of regenerated energy during braking, to then utilize it during accelerations. This could potentially lead to significant reductions in fuel consumption, cutting both costs and environmental impact.
- **Improved transient performance** - Without energy storage the power produced by the ICE has to go either to traction, external consumers or to increasing shaft speed or voltage. In a case when there is no external consumption and the shaft speed and voltage references are constant, all power from the ICE has to go to traction. In this way, any irregularity in ICE power (for example due to turbo lag) will propagate to the TM. If an energy storage would be present, power could be provided from this component in order to achieve smoother transients.
- **Increased braking capacity** - In the studied powertrain, braking without using the mechanical brakes is limited to engine braking, and even at the maximum speed of the engine, the engine braking power is only approximately 29 kW. If energy storage was possible, the braking capacity could be significantly increased by charging the storage with regenerated power from the TM. This would spare the mechanical brakes and thus reduce maintenance costs.

Additionally, adding this component would also make other control strategies possible. For example, recall Figure 6.2 where the power paths through the DC bus are analyzed. If an energy storage was present, CS2 could possibly be feasible since the problems encountered at standstill and no traction demand could be handled with this energy storage.

9

Conclusions & Future Work

9.1 Conclusions

In this section the conclusions drawn from the thesis are summarized. These conclusions are presented together with the questions in Section 1.3 in order to reconnect to the initial problem formulation.

How can a control system working according to the proposed strategy be realized?

The proposed control strategy in its original form (CS2) is not feasible due to the inability to achieve voltage control using the TM when 1) the vehicle stands still, and 2) the driver demands no traction. Tweaking CS2 to handle these corner cases is difficult in practice since both voltage and speed control are realized on subcomponent level in the TCU and GCU respectively, greatly limiting the control design possibilities. However, alternative approaches still working according to the push principle are possible, for example by migrating control loops from the subcomponent control units to the PCM.

In this thesis, a working push control strategy is developed and presented. This strategy proves that it is possible to successfully control a diesel-electric powertrain according to the push principle.

Which advantages and disadvantages does the proposed control strategy possess?

The identified advantages and disadvantages with the push approach are listed below.

- Using the push control approach solves the original problem with maximum utilization of the available engine power, potentially allowing for

downsizing of the installed engine.

- A push control strategy naturally handles load prioritization in the case when external loads have higher priority than traction, without the need to implement any priority-specific logic.
- Takeoff and slow speed driving are problematic by design due to the varying effective gear ratio which grows to infinity when the vehicle speed approaches zero. This implies that even the smallest possible increase in ICE torque will cause the TM to generate maximum torque at standstill. Hence, a deliberate takeoff strategy is crucial in order to handle this characteristic.
- In the push principle the driver controls the ICE instead of the TM, while the TM controls the engine speed (in the case of the developed CS3). This approach gives the driver only indirect control of the traction torque, and makes dynamics from the speed control affect the traction. This might cause bumpy acceleration of the vehicle and is thus disadvantageous from a drivability perspective. Furthermore, this puts high demands on the speed reference selection algorithm which plays a critical role in counteracting this undesired bumpiness.

Are there other control strategies that are worth considering for this application?

During the work, no other alternative control approaches have been identified.

9.2 Future work

With the developed control strategy, powertrain control according to the push approach can be realized. This brings the benefit of potential reduction in installed engine size, which enables several advantages. Since some problematic characteristics have been identified with this approach, further work is needed in order to improve the developed strategy and make it practically applicable. Such prospective areas of improvement are presented below.

9.2.1 Speed reference selection algorithm

The speed reference selection algorithm is of major importance for achieving smooth traction. In this thesis a rather basic algorithm is applied, so developing a more sophisticated one could improve performance significantly. Below, some ideas for further improvement of this algorithm are presented.

- Achieve movement of the operating point in the engine map in a more optimal manner during transients, maybe as described in [16].
- Sustain a high engine speed reference during engine braking to maximize engine braking power.

- Choose the proportion of produced ICE torque allowed for shaft acceleration β in a dynamic, more refined way.
- Instead of using an operating point map where the desired engine speed changes continuously with requested power (as in this thesis), the engine speed reference could be fixed in discrete intervals, imitating the gears of a gearbox. It is conceivable that this technique could reduce the traction bumpiness since speed reference changes, which are the main causes for the bumps, would occur less often.

9.2.2 Takeoff strategy

Having a well-functioning takeoff strategy is important in order to enable satisfactory low speed driving. Three possible approaches have been identified in the thesis, of which only one is tested. It would be interesting to see a deeper analysis of this topic, both evaluating the identified approaches and generating other, more advanced concepts. One prospective takeoff technique that is considered particularly interesting is using the pull principle at low vehicle speeds, to then perform a mode switch to the push principle when the speed increases.

9.2.3 Improved model validation

As no measurement data from the real powertrain has been available, the possibility to perform adequate validation of the developed model has been limited. Thus, it would be highly relevant to perform such validation as measurements become available.

9.2.4 Extended fictive drive cycle

In the thesis, a considerably simplified drive cycle is used to evaluate the control strategy. Extending this drive cycle to incorporate more load cases (for example by introducing AUX and PAR loads at 0% and 50% traction power) could reveal further characteristics of the strategy.

Bibliography

- [1] SAE J1939 standard, accessed 2018-04-04. URL https://www.sae.org/standards/content/j1939_201308/. Cited on pages 8, 26, and 30.
- [2] Stefano Barsali, Massimo Ceraolo, and Andrea Possenti. Techniques to control the electricity generation in a series hybrid electrical vehicle. *IEEE Transactions on Energy Conversion*, 17(2):260–266, 2002. Cited on page 19.
- [3] S. Chandra and M.M. Agarwal. *Railway Engineering*. Oxford University Press, 2007. Cited on page 19.
- [4] Linköping University Vehicular Systems division. Software, 2018. URL <http://www.vehicular.isy.liu.se/Software/>. Cited on page 15.
- [5] Mehrdad Ehsani, Gao Yimin, Sebastien E. Gay, and Ali Emadi. *Modern Electric, Hybrid Electric, and Fuel Cell Vehicles: Fundamentals, Theory and Design*. CRC Press LLC, 2005. Cited on page 19.
- [6] Lars Eriksson and Lars Nielsen. *Modeling and Control of Engines and Drivelines*. John Wiley & Sons, 2014. Cited on pages 21 and 25.
- [7] R.D. Geertsma, R.R. Negenborn, K. Visser, and J.J. Hopman. Design and control of hybrid power and propulsion systems for smart ships: A review of developments. *Applied Energy*, 194, 2017. Cited on page 20.
- [8] Jan Fredrik Hansen and Frank Wendt. History and state of the art in commercial electric ship propulsion, integrated power systems, and future trends. *Proceedings of the IEEE*, 103(12), 2015. Cited on page 20.
- [9] Jan Fredrik Hansen, Alf Kåre Ådnanes, and I. Fossen Thor. Mathematical modelling of diesel-electric propulsion systems for marine vessels. *Mathematical and Computer Modelling of Dynamical Systems*, 7(1), 2001. Cited on page 21.
- [10] Amir Khajepour, Saber Fallah, and Avesta Goodarzi. *Electric and hybrid vehicles: technologies, modeling and control: a mechatronic approach*. John Wiley & Sons, 2014. Cited on page 19.

- [11] Werner Leonhard. *Control of Electrical Drives*. Springer-Verlag Berlin Heidelberg, 2nd edition, 1996. Cited on page 9.
- [12] Chris Mi, M. Abul Masrur, and David Wenzhong Gao. *Hybrid Electric Vehicles: Principles and Applications with Practical Perspectives*. John Wiley & Sons, 2011. Cited on page 19.
- [13] V. Nezhadali, M. Sivertsson, and L. Eriksson. Turbocharger dynamics influence on optimal control of diesel engine powered systems. *SAE International Journal of Engines*, 7(1), 2014. Cited on page 20.
- [14] M. Sivertsson and L. Eriksson. Optimal and real-time control potential of a diesel electric powertrain. *Proceedings of the 19th IFAC World Congress, Cape Town, South Africa*, 2014. Cited on page 51.
- [15] M. Sivertsson and L. Eriksson. Modeling for optimal control: A validated diesel-electric powertrain model. *SIMS2014 - 55th International Conference on Simulation and Modelling, Aalborg, Denmark*, 2014. Cited on pages 15, 21, 23, and 25.
- [16] M. Sivertsson and L. Eriksson. Optimal transient control trajectories in diesel–electric systems—part i: Modeling, problem formulation, and engine properties. *Journal of Engineering for Gas Turbines and Power*, 137(2), 2015. Cited on pages 21 and 72.
- [17] M. Sivertsson and L. Eriksson. Optimal transient control trajectories in diesel–electric systems—part ii: Generator and energy storage effects. *Journal of Engineering for Gas Turbines and Power*, 137(2), 2015. Cited on page 21.
- [18] Asgeir J. Sørensen and Øyvind N. Smogeli. Torque and power control of electrically driven marine propellers. *Control Engineering Practice*, 17, 2009. Cited on page 20.
- [19] Stefan Östlund. *Electrical Machines and Drives*. KTH Electrical Machines and Power Electronics, 2009. Cited on page 9.
- [20] J. Wahlström and L. Eriksson. Modelling diesel engines with a variable-geometry turbocharger and exhaust gas recirculation by optimization of model parameters for capturing non-linear system dynamics. *Proceedings of the Institution of Mechanical Engineers, Part D, Journal of Automobile Engineering*, 225(7), 2011. Cited on page 21.